# ITS1 metabarcoding highlights low specificity of lichen mycobiomes at a local scale

Fernando Fernández-Mendoza[1] | Antonia Fleischhacker[1] | Theodora Kopun[1] | Martin Grube[1] | Lucia Muggia[2]

[1]Institute of Plant Sciences, Karl-Franzens-University Graz, Graz, Austria

[2]Department of Life Sciences, University of Trieste, Trieste, Italy

**Correspondence**
Lucia Muggia, Department of Life Sciences, University of Trieste, Trieste, Italy.
Email: lmuggia@units.it

**Funding information**
Austrian Science Fund, Grant/Award Number: P24114-B16, P26359

## Abstract

As self-supporting and long-living symbiotic structures, lichens provide a habitat for many other organisms beside the traditionally considered lichen symbionts—the myco- and the photobionts. The lichen-inhabiting fungi either develop diagnostic phenotypes or occur asymptomatically. Because the degree of specificity towards the lichen host is poorly known, we studied the diversity of these fungi among neighbouring lichens on rocks in an alpine habitat. Using a sequencing metabarcoding approach, we show that lichen mycobiomes clearly reflect the overlap of multiple ecological sets of taxa, which differ in their trophic association with lichen thalli. The lack of specificity to the lichen mycobiome is further supported by the lack of community structure observed using clustering and ordination methods. The communities encountered across samples largely result from the subsampling of a shared species pool, in which we identify three major ecological components: (i) a generalist environmental pool, (ii) a lichenicolous/endolichenic pool and (iii) a pool of transient species. These taxa majorly belong to the fungal classes Dothideomycetes, Eurotiomycetes and Tremellomycetes with close relatives in adjacent ecological niches. We found no significant evidence that the phenotypically recognized lichenicolous fungi influence the occurrence of the other asymptomatic fungi in the host thalli. We claim that lichens work as suboptimal habitats or as a complex spore and mycelium bank, which modulate and allow the regeneration of local fungal communities. By performing an approach that minimizes ambiguities in the taxonomic assignments of fungi, we present how lichen mycobiomes are also suitable targets for improving bioinformatic analyses of fungal metabarcoding.

**KEYWORDS**
Chaetothyriales, Dothideomycetes, endolichenic, lichenicolous, symbiosis, Tremellales

## 1 | INTRODUCTION

Lichens are symbiotic systems formed by the association of biotrophic fungi with populations of one or more phototrophic microorganisms, usually green algae and/or cyanobacteria. The interaction of compatible partner organisms results in the development of self-sustaining and long-living structures, the lichen thallus, in which the primary producers are sheltered extracellularly in a matrix of fungal hyphae (Hawksworth & Honegger, 1994). These structures are not closed and provide habitats suitable for the colonization by other organisms, such as (noncyanobacterial) prokaryotes (Aschenbrenner, Cernava, Berg, & Grube, 2016; Bates, Cropsey, Caporaso, Knight, & Fierer, 2011; Bates, Walters, Knight, & Fierer, 2012; Cardinale, Vieira de Castro, Müller, Berg, & Grube, 2008; Grube, Cardinale, Vieira de

Castro, Müller, & Berg, 2009; Grube et al., 2015) and additional fungi (Fleischhacker, Grube, Kopun, Hafellner, & Muggia, 2015; Lawrey & Diederich, 2003; Muggia, Fleischhacker, Kopun, & Grube, 2016; Muggia & Grube, 2010; Spribille et al., 2016).

The presence of lichenicolous fungi, literally, fungi on lichens, has been long acknowledged in the literature (Lawrey & Diederich, 2003, 2017). They were even recognized before the symbiotic nature of lichens was discovered, because they can develop recognizable reproductive structures, or cause conspicuous symptoms on their hosts, such as gall-like hypertrophisms or local discolorations (Lawrey & Diederich, 2003). Many of the known 1800 lichenicolous species are only weak parasite, which take long-term benefit from the functional symbiosis of the host organisms, but there are also more pathogenic species which destroy their hosts.

Even though attempts to culture lichenicolous fungi date back to the last century (Crittenden, David, Hawksworth, & Campbell, 1995), they became only more recently a basis for their phylogenetic analysis (e.g., Ertz et al., 2015, 2016; Lawrey, Etayo, Dal-Forno, Driscoll, & Diederich, 2015; Lawrey, Zimmermann, Sikaroodi, & Diederich, 2016; Muggia, Kopun, & Ertz, 2015). Culturing material of lichens, however, also revealed another fraction of barely visible lichenicolous fungi (Girlanda, Isocrono, Bianco, & Luppi-Mosca, 1997; Petrini, Hake, & Dreyfuss, 1990; Prillinger et al., 1997). These studies did not properly discriminate between surface and inner parts of the lichens, but later studies confirmed that additional fungi also occur without symptoms internally in lichen thalli. For the analogy with endophytes, these fungi were called 'endolichenic fungi' (Arnold et al., 2009; Chagnon, U'Ren, Miadlikowska, Lutzoni, & Elizabeth Arnold, 2016; Fleischhacker et al., 2015; Muggia et al., 2016; U'Ren, Lutzoni, Miadlikowska, & Arnold, 2010; U'Ren, Lutzoni, Miadlikowska, Laetsch, & Arnold, 2012).

A remaining limitation of the culture-dependent approaches is the underrepresentation of species, which depend on the host structures and, generally, of slow-growing species that are outcompeted under the culturing conditions (U'Ren et al., 2014). It is therefore not surprising that modern sequencing approaches detect a much higher diversity of the lichen mycobiome than culture-dependent approaches or morphological analyses (Wang, Zheng, Wang, Wei, & Wei, 2016; Zhang, Wei, Zhang, Liu, & Yu, 2015). Lately, a transcriptomic approach detected previously unrecognized basidiomycete yeasts as a common component of the upper surface layer in a lichen family (Spribille et al., 2016).

In this study, we used 454 pyrosequencing to study the diversity of the lichen mycobiome taking in account lichen thalli which presented visible infections by lichenicolous fungi and thalli devoid of visible fungal infections (Fleischhacker et al., 2015; Muggia et al., 2016) in a subalpine, rock habitat in the Eastern Alps. We evaluated (i) whether lichenicolous fungi can be found asymptomatic in typical and atypical lichen hosts, (ii) the diversity and (iii) the specificity of the lichen mycobiome among and towards different lichen hosts, respectively, (iv) whether symptomatic lichenicolous infections affect the diversity of the other intrathalline, cryptically occurring fungi.

## 2 | MATERIALS AND METHODS

### 2.1 | Sampling

Lichen samples were collected in ten plots (each of about 300 $m^2$) at an altitude of 1800–1900 m, on the Koralpe mountain range in Eastern Austria. As part of a wider study of fungal communities (Fleischhacker et al., 2015; Muggia et al., 2016), 26 samples of crustose lichens (i.e., composed by contiguous areoles tightly adhered to the substrate) characteristic for alpine rock communities were selected. Half of the samples (13) were thalli infected by lichenicolous fungi, including Coelomycetes, teleomorphic and anamorphic Ascomycetes (Figure 1, Table 1) that could be identified by morphological analyses. All together, the data set includes 12 species of lichenicolous fungi and 13 species of lichen hosts (Table 1).

### 2.2 | DNA extraction, amplification and sequencing

The lichen material was physically cleaned using a brush and double distilled water, detached from the rock substrate with a sterile razor blade, transferred to 1.5-ml reaction tubes and air-dried. We could not surface-sterilize the material as proposed in other surveys, as crustose lichens, being tightly adhered to the substrate, lack a lower cortex and have an intricate system of thalline areoles and margins (prothallus) that cannot be properly sterilized by chemical methods without disrupting the whole sample itself. Furthermore, the difference of what is within and around the lichen thallus is not clear in all samples, making the choice of surface to sterilize arbitrary. Therefore, we took particular care in excising from the thallus only a single part, either bearing the lichenicolous fungal infection for the infected thalli, or an areola central in the thallus for the specimens devoid of any sign of fungal infection.

The dry material was frozen (−80°C), ground to powder using a TissueLyserII (Retsch). DNA extractions were carried out with the DNeasy Plant Mini Kit (Qiagen, Austria). The nuclear ribosomal ITS region was amplified using fungal-specific primers ITS1F (Gardes & Bruns, 1993) and ITS2 (White, Bruns, Lee, & Taylor, 1990), which amplify the ITS1 spacer region of about 300 bp of length (as part of the ITS fungal barcode, Schoch et al., 2012), suitable for amplicon sequencing using Roche's 454 platform. We have here focused on ITS1, for an expected higher resolution of this region. Irrespective of discussions about the better suitability of ITS regions, each locus introduces a bias, so different barcode and primers are expected to render different results (Bellemain et al., 2010; Schmidt et al., 2013). As long as the bias is systematic, samples are still comparable, although the composition of the mycobiomes cannot be discussed in absolute terms. Furthermore, it has been confirmed by Blaalid et al. (2013) that either region to large extent yield similar results. PCRs were performed in triplicates of 25 μl reaction volumes, containing ca. 20 ng of DNA template and 5 pmol of each forward and reverse amplicon primers. The forward primer was tagged with a different multiplex identifier (MID) for each sample. Amplification was performed with the FastStart High Fidelity PCR System (Roche Diagnostics) as described

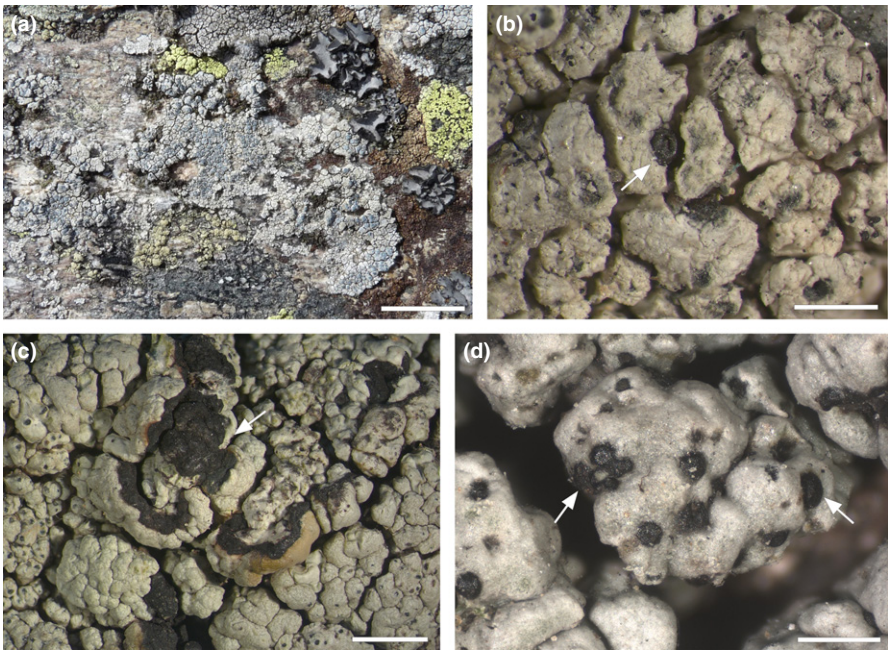


**FIGURE 1** (a) Alpine community of rock inhabiting lichens. (b–d) Lichenicolous fungi on lichen host thalli: (b) *Sagediopsis fissurisedens* on *Aspilidia myrinii*, (c) *Taeniolella atricerebrina* on *Tephromela atra*, (d) *Muellerella atricola* on *Tephromela atra*. Arrows indicate the recognizable, phenotypic characters of the lichenicolous fungi: (b) perithecia at the margins of thallus areoles, (c) cecidiogeneous, melanized galls containing conidiogeneous cells, (d) perithecia immersed in thallus areoles. Scale bars: a = 4 cm, b = 1 mm, c = 2 mm, d = 0.5 mm

and published in Kozich, Westcott, Baxter, Highlander, and Schloss (2013). PCR conditions were as follows: the initial denaturation for 3 min at 95°C was followed by 32 cycles of 45 s denaturation at 95°C, 45 s annealing at 50°C, 1 min extension at 72°C and a final extension step at 72°C for 7 min. The triplicates were pooled after PCR amplification. PCR products were checked on a 1% agarose gel (5 μl sample, 25 min, 120 V). When found, bands of different sizes were individually excised from the gel and cleaned separately with the E.Z.N.A.® MicroElute Gel Extraction Kit (Omega bio-tech, VWR). Amplicons were additionally purified using a denaturing HPLC on a WAVE apparatus (Transgenomic, Inc., Omaha, NE, USA), eluted in 30 μl elution buffer (Qiagen, Hilden, Germany) and quantified using the Quant-iT™ PicoGreen® dsDNA Assay Kit (Life Technologies, CA, USA). Emulsion PCR of the samples pooled in equimolar concentration was performed using the GS Titanium MV emPCR Kit and method (Lib-L) (Roche 454 Life Science, Branford, CT, USA) according to manufacturer's instructions, and sequencing was performed using the GS FLX Titanium Sequencing Kit XLR70 (Roche 454 Life Science, Branford, CT, USA). A negative control was run together starting from the DNA extraction and was confirmed to be negative during the whole processing (lack of amplicons after PCR and sequencing).

## 2.3 | Preprocessing of 454 amplicons

Binary files were processed to obtain fastq files in the sequencing facility. Quality-fasta files were processed in Acacia v.1.5.2 (Bragg, Stone, Imelfort, Hugenholtz, & Tyson, 2012) to interpret and remove MID tags, to denoise and to quality filter the amplicon sequences. Reads shorter than 150 bp and those outside of a read length interval centred on the average read length plus and minus two standard deviations were excluded for further use. Also, sequences with an average quality score below 20, as well as those including an ambiguity within the first 350 bp, were excluded from further use. Error correction used a Balzer model to account for asymmetry in under-calls and over-calls. (Rn-length encoding (RLE) sequences were decomposed in hexamers and clustered using a single-linkage approach. We clustered sequences that did not exceed a Manhattan distance threshold of 13, for instance two internal insertion/deletion errors and an end insertion/deletion. Finally, for each "cluster" of corrected sequences, Acacia provided a modal representative sequences. These are passed on to fasta files with replication information on the header and sorted by sampling location using the SNOWMAN pipeline version 1.21 (Halwachs et al., 2013).

The unique amplicon files per sample were blasted using BLASTN 2.2.30 (Zhang, Schwartz, Wagner, & Miller, 2000) against a local copy of the NCBI nucleotide (nt) database (updated 4 April 2015). Output files were batch processed to generate raw taxonomic profiles based on the lowest common-ancestor (LCA) algorithm implemented in *Megan* v.5.10.2 (Huson, Mitra, & Ruscheweyh, 2011) using a bit-score threshold of 200 and otherwise default settings with the minimum support per cent turned off. The resulting.*rma* files were combined to allow the taxonomic comparison of samples. This method maximizes the number of amplicons used but increases the taxonomic bias for some fungal groups due to the confounding phylogenetic signal generated by the presence of group I intron at the end of the nuclear small ribosomal subunit (nucSSU). Further, this presence of the group I intron strongly reduced the actual coverage of ITS1. Nevertheless, the majority of the studied amplicons comprised partial sequences of the ITS1 region.

The whole analytical pipeline performed in this study is schematically reported in the Fig. S1.

## 2.4 | ITS1 data set assembly

Unique amplicon files were filtered using *ITSx* (Bengtsson-Palme et al., 2013) to identify fungal ribosomal regions and extract only

**TABLE 1** Summary of the experimental set-up and sequencing results. Samples are ordered according to the presence or absence of symptomatic lichenicolous fungi and alphabetically by the name of the lichen host. The table includes the following: samples numbers, the scientific names of the hosts and the afore known lichenicolous fungus when present, the total number of reads (total), the number of unique dereplicated sequences, the number of reads containing the fungal ITS1 region as identified by *ITSx*, the number of ITS1 reads excluding those of the lichen host and the number of reads of the final data set which also excludes reads blasting to other lichen species found in the community. It further reports the sample-specific threshold used to interpret the community tables use for network analyses, that is the averaged value of the proportion of ITS1 reads per sample belonging to contaminant lichen and fungal species, and in brackets, the same average proportion but of the complete data set. The number of MOTUs/sample as identified using *swarm* (total), the number of MOTUs other than the lichen host (not lichen) and the number of nonsingleton MOTUs (not single) are also reported

| | | | Reads | | | | | | ITS1 OTUs | | |
|---|---|---|---|---|---|---|---|---|---|---|---|
| Sample | Lichen host | Infecting fungus | Total | Unique | ITS1 | Not lichen | Final | Threshold % | Total | Not lichen | Not single |
| A623 | *Acarospora fuscata* | – | 936 | 544 | 52 | 51 | 19 | 0.2895 (0.0059) | 29 | 28 | 14 |
| A420 | *Aspilidea myrinii* | – | 981 | 122 | 968 | 52 | 50 | 0.04 (0.002) | 109 | 24 | 22 |
| A138 | *Candelariella vitellina* | – | 1452 | 405 | 1194 | 211 | 177 | 0.048 (0.0059) | 186 | 83 | 75 |
| A368 | *Lecanora bicincta* | – | 1764 | 283 | 1678 | 16 | 16 | 0.001 (0.001) | 206 | 6 | 6 |
| A360 | *Lecanora intricata* | – | 7081 | 2060 | 5302 | 5228 | 5222 | 0.0011 (0.001) | 898 | 887 | 885 |
| A243 | *Lecanora polytropa* | – | 3332 | 933 | 2549 | 2547 | 2541 | 0.0012 (0.001) | 339 | 337 | 333 |
| A227 | *Lecanora swartzii* | – | 8699 | 1897 | 6250 | 6249 | 6229 | 0.001 (0.001) | 481 | 480 | 473 |
| A792 | *Lecidea lapicida* | – | 6500 | 1052 | 5994 | 983 | 914 | 0.0022 (0.001) | 642 | 278 | 230 |
| A229 | *Psorinia conglomerata* | – | 4854 | 1100 | 4540 | 58 | 53 | 0.0314 (0.001) | 809 | 26 | 21 |
| A476 | *Psorinia conglomerata* | – | 1673 | 357 | 1504 | 495 | 482 | 0.027 (0.0078) | 232 | 88 | 84 |
| A172 | *Rhizocarpon geographicum* | – | 4919 | 847 | 4721 | 183 | 175 | 0.0229 (0.001) | 652 | 39 | 37 |
| A361 | *Tephromela atra* | – | 8716 | 2068 | 6306 | 6304 | 6266 | 0.002 (0.0015) | 843 | 841 | 832 |
| A032 | *Umbilicaria cylindrica* | – | 4372 | 1316 | 3171 | 3145 | 2744 | 0.0244 (0.0153) | 498 | 491 | 439 |
| A608 | *Aspilidea myrinii* | *Sagediopsis fissurisedens* | 6007 | 962 | 5750 | 1257 | 1229 | 0.0038 (0.001) | 723 | 331 | 325 |
| A832 | *Lecanora bicincta* | *Arthonia varians* | 4185 | 698 | 3922 | 306 | 274 | 0.1168 (0.0076) | 461 | 65 | 61 |
| A482 | *Lecanora polytropa* | *Cercidospora epipolytropa* | 2478 | 1061 | 1420 | 1381 | 1377 | 0.0015 (0.001) | 315 | 291 | 289 |
| A418 | *Lecanora polytropa* | *Lichenoconium lecanorae* | 1216 | 291 | 1113 | 59 | 58 | 0.0172 (0.001) | 188 | 21 | 20 |
| A434 | *Lecanora polytropa* | *Lichenoconium lecanorae* | 1131 | 359 | 991 | 990 | 930 | 0.0129 (0.0106) | 220 | 219 | 206 |
| A670 | *Lecanora polytropa* | *Muellerella pygmaea-Lp* | 3646 | 1176 | 2595 | 2594 | 2589 | 0.001 (0.001) | 425 | 424 | 420 |
| A636 | *Lecidea lapicida* | *Muellerella pygmaea s.s.* | 4652 | 648 | 4272 | 82 | 82 | 0.001 (0.001) | 364 | 28 | 28 |
| A194 | *Rhizocarpon geographicum* | *Endococcus macrosporus* | 5473 | 1261 | 4965 | 1113 | 1110 | 0.0027 (0.001) | 875 | 227 | 224 |
| A405 | *Rhizocarpon geographicum* | *Muellerella pygmaea-Rg* | 1208 | 149 | 1179 | 2 | 2 | 0.001 (0.001) | 120 | 2 | 2 |
| A440 | *Tephromela atra* | *Muellerella atricola* | 1246 | 373 | 1105 | 1105 | 1077 | 0.026 (0.0225) | 246 | 246 | 244 |
| A280 | *Tephromela atra* | *Skyttea tephromelarum* | 8750 | 2567 | 5912 | 5906 | 5888 | 0.001 (0.001) | 880 | 877 | 867 |
| A809 | *Tephromela atra* | *Taeniolella atricerebrina* | 6446 | 1739 | 5347 | 5347 | 5330 | 0.001 (0.001) | 897 | 897 | 886 |
| A622 | *Varicellaria lactea* | *Stigmidium eucline* | 5701 | 1541 | 4628 | 2985 | 2952 | 0.0028 (0.0014) | 886 | 434 | 424 |
| | | Maximum | 8750 | 2567 | 6306 | 6304 | 6266 | 0.289 | 898 | 897 | 886 |
| | | Average | 4131 | 993 | 3363 | 1871 | 1838 | 0.027 | 482 | 295 | 286 |
| | | Minimum | 936 | 122 | 52 | 2 | 2 | 0.001 | 29 | 2 | 2 |

those fragments identified as fungal ITS1. By eliminating those reads and parts of the reads not identified as fungal ITS1, we reduced the biases introduced using different loci in an alignment-based taxonomic assignment. Such stringent filtering of the data set had a negative consequence on the effective depth of the study due to the high proportion of reads including the group I intronic region (Figure 2, Table 1). The ITS1 fractions were clustered into molecular operational taxonomic units (MOTUs) using the single-linkage clustering method implemented in *swarm* (Mahé, Rognes, Quince, de Vargas, & Dunthorn, 2014) using threshold d = 1 and the *fastidious* option to reduce the number of smaller MOTUs while maintaining a high clustering resolution. In this process, chimeric sequences were also identified and excluded.

The taxonomic assignment of ITS1 MOTUs was carried out by blasting the reference sequence of each MOTU against a local database created from UNITE+INSDC (Abarenkov et al., 2010) release 7 (downloaded

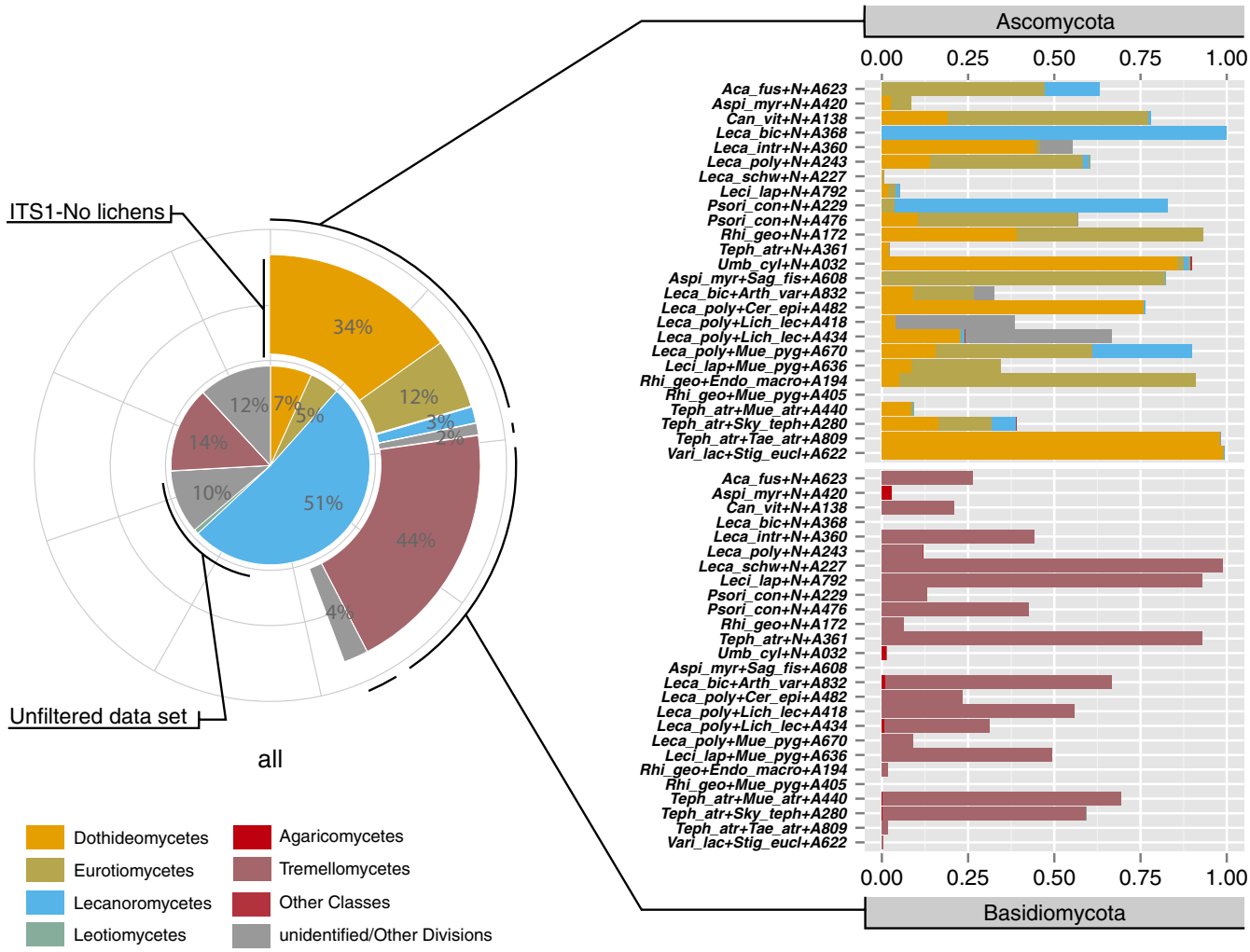


**FIGURE 2** Taxonomic composition of the ITS1 data set at division level. On the left, global pie chart showing the difference of read amount considering the full and the lichen mycobiont-trimmed ITS1 datasets (left). On the right, abundance plot at fungal division level (Ascomycota and Basidiomycota) for each sample

4 April 4 2015). The *blastn* tabular output (-outfmt 10) including all accessions with an alignment e-value above the fixed threshold of $5 \times 10^{-4}$ was processed using custom scripts (see data accessibility section) to parse, tabulate the taxonomic information and summarize the taxonomic assignment for each MOTU independently at division, class, order, family and genus levels (Appendix S1). For each category, we used the known taxonomic assignment with the minimum e-value. A pseudospecies category was used to identify the lowest taxonomic category with the lowest e-value. The consistence of the taxonomic assignment was graphically explored for the most frequent MOTUs using boxplots. For each MOTU, a plot was generated for each taxonomic category (division, class, order, family, genera and "pseudospecies") using the e-values of each blast hit sorted by taxonomic assignment. Boxplots can be found in the github repository referred in the Data Accessibility section.

To specifically study the diversity patterns and composition of the lichen mycobiome in the further analyses, MOTUs belonging to the lichen mycobiont of each sample were filtered out of the ITS1 data set (Figure 2, Table 1). We also realized that there was a widespread presence of MOTUs identifiable as lichen mycobionts in all samples. Most were the same lichen mycobiont species of the samples used in the study as part of the local community, while other belonged to lichen mycobionts that, when present, may be found at lower elevations. Such MOTUs identified as lichen mycobionts other than those of our analysed samples were also queried out. The data set in the shape of reads per sample and MOTU was not normalized to obtain rarefied estimates of MOTU richness for each sample. Alternatively, for further use, the data set was normalized as the proportion of the total number of reads per sample represented by each MOTU.

## 2.5 | Lichenicolous fungi identification and phylogenetic analyses

The MOTUs assigned to identifiable lichenicolous fungi, after having checked their identity by blast analyses, were manually extracted of the complete MOTU data set (Table 2, Appendix S1). Individual alignments of the ITS1 sequences were carried out for each identified lichenicolous fungus using MAFFT (Katoh, 2013), using an

automatic algorithm choice and default settings; alignments were later corrected manually in BioEdit (Hall, 1999). In each alignment, we included the newly generated ITS1 sequences and any sequence from lichenicolous species or of the closest related species already available in the GenBank database. Single locus data sets were analysed with a maximum-likelihood (ML) approach using the RAXML GUI program (v 1.5, Stamatakis, 2004, 2006; Silvestro & Michalak, 2011). A GTR+GAMMA model was used, and 1000 bootstrap replicates were run. The phylogenetic trees were visualized in FIGTREE v.1.4 (available from: http://tree.bio.ed.ac.uk/software/figtree).

## 2.6 | Statistical analyses

All statistical analyses and data manipulation were carried out in R v. 3.0.3 (R Development Core Team 2011). For the description of quantitative networks, we used the R package BIPARTITE (Dormann, Fründ, Bluthgen, & Gruber, 2009; Dormann, Gruber, & Fründ, 2008), while package CIRCLIZE (Gu, Gu, Eils, Schlesner, & Brors, 2014) was used for the graphical representation of networks at sample level (Figures 3 and 4). For the description of diversity and community structure, we used packages VEGAN (Oksanen et al., 2015) and MCLUST v. 4.4 (Fraley & Raftery, 2002; Fraley, Raftery, Murphy, & Scrucca, 2012).

## 2.7 | Uni- and bipartite sample networks and threshold filtering

Uni- and bipartite networks were generated to visualize differences in the diversity and the specificity of the mycobiomes in the lichen samples. The ITS1 data set was tabulated as reads/MOTU and reads/sample and was normalized using sample totals (Table 3). The Table 3 was used to generate unipartite and bipartite (sample-MOTU) networks at sample level. Separate networks were further obtained for the complete data set using each of the four most represented fungal orders recovered: Botryosphaeriales, Capnodiales, Chaetothyriales and Tremellales.

**TABLE 2** Summary of the main MOTUs and the number of their corresponding reads identified as the lichen hosts, the symptomatic lichenicolous fungi and other relevant fungi per sample

| Sample | Lichen host | OTU (Reads) | Infecting fungus | OTU (Reads) | Other relevant fungi OTU (Reads) |
|---|---|---|---|---|---|
| A623 | *Acarospora fuscata* | – (874) | – | | |
| A420 | *Aspilidea myrinii* | 5 (916) | – (*Sagediopsis fissurisedens*) | 34 (2) | |
| A138 | *Candelariella vitellina* | 25 (920) | – | | |
| A368 | *Lecanora bicincta* | 9 (1635) | – | | |
| A360 | *Lecanora intricata* | – (1283) | – | | 13 (1533) Tremellales, 14 (1335) Capnodiales |
| A243 | *Lecanora polytropa* | – (379) | – (*Muellerella pygmaea*) | 21 (586) | |
| A227 | *Lecanora swartzii* | – (2273) | – | | |
| A792 | *Lecidea lapicida* | 4 (4971, *Lecanora*) | – | | |
| A229 | *Psorinia conglomerata* | 11 (4303) | – | | |
| A476 | *Psorinia conglomerata* | 19 (958) | – | | |
| A172 | *Rhizocarpon geographicum* | 2 (3466) | – | | |
| A361 | *Tephromela atra* | – (1327) | – | | |
| A032 | *Umbilicaria cylindrica* | – (963) | – | | 20 (1067) Botryosphaeriales |
| A608 | *Aspilidea myrinii* | 5 (4493) | *Sagediopsis fissurisedens* | *34 (858)* | |
| A832 | *Lecanora bicincta* | 9 (3523) | *Arthonia varians* | *– (–)* | 1 (177) Tremellomycetes |
| A482 | *Lecanora polytropa* | – (830) | *Cercidospora epipolytropa* | *18 (990)* | 26 (287) Tremellomycetes |
| A418 | *Lecanora polytropa* | 16 (965) | *Lichenoconium lecanorae* | *32 (18)* | |
| A434 | *Lecanora polytropa* | – (64) | *Lichenoconium lecanorae* | *32 (378)* | |
| A670 | *Lecanora polytropa* | – (729) | *Muellerella pygmaea-Lp* | *21 (1033)* | |
| A636 | *Lecidea lapicida* | 6 (4113) | *Muellerella pygmaea s.s.* | *21 (11)* | |
| A194 | *Rhizocarpon geographicum* | 8 (3701) | *Endococcus macrosporus* | *17 (933)* | |
| A405 | *Rhizocarpon geographicum* | 15 (1161) | *Muellerella pygmaea-Rg* | *– (24)* | |
| A440 | *Tephromela atra* | – (44) | *Muellerella atricola* | *46 (164)?* | |
| A280 | *Tephromela atra* | – (2102) | *Skyttea tephromelarum* | *33 (411)* | |
| A809 | *Tephromela atra* | – (652) | *Taeniolella atricerebrina* | *10 (4537)* | |
| A622 | *Varicellaria lactea* | 22 (1551) | *Stigmidium eucline* | *12 (2826)* | |

The number of reads identified for the symptomatic lichenicolous fungus is reported in italics.

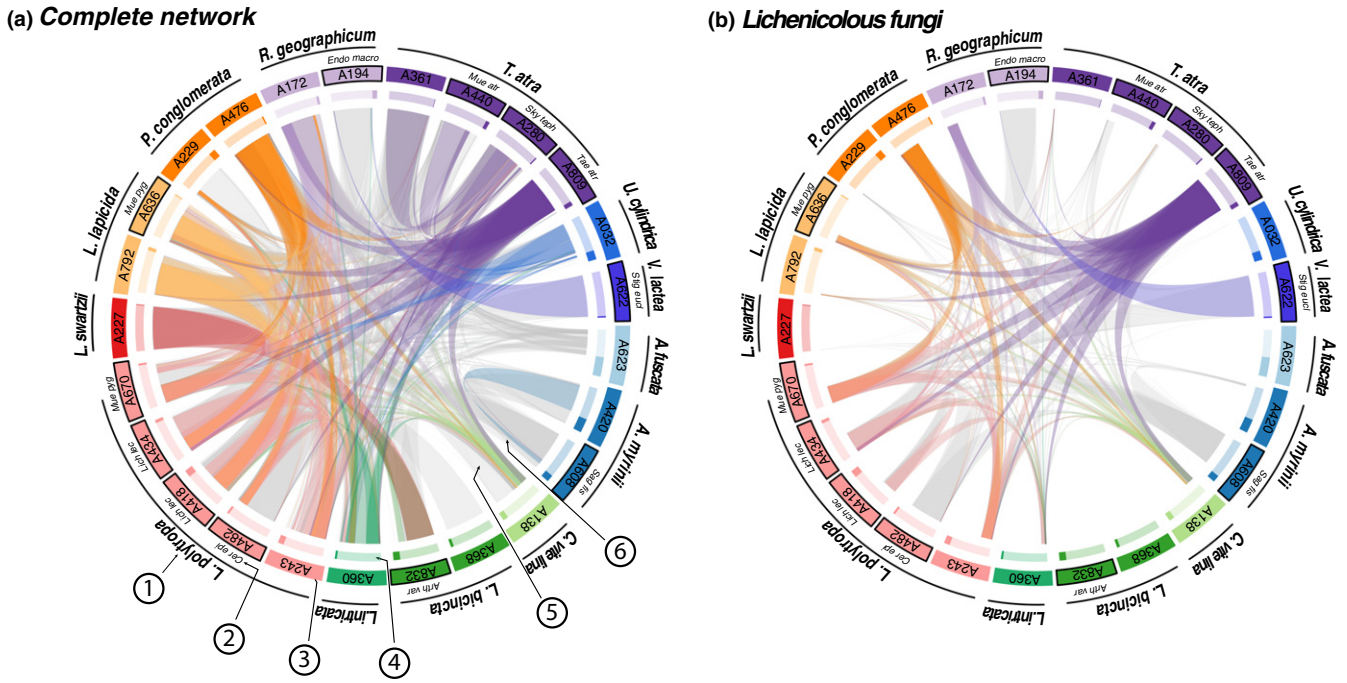


**FIGURE 3** Circos plot summarizing uni- and bipartite networks for (a) the complete data set and (b) the data set using only the main lichen-associated fungi MOTUs. The numbering 1–6 indicates: (1) the names of lichen hosts; (2) the name of the symptomatic lichenicolous fungus (when present) abbreviated to the first three letters of the genus and of the species names (for reference use Table 1); (3) alphanumeric sample number, different colours distinguish samples for which the lichen mycobiont is the same, the black margin further highlights those samples presenting a symptomatic lichenicolous fungus; (4) percentage of reads belonging to shared (light) and exclusive (dark) MOTUs for each sample in the nonthresholded data set - the connectors represent MOTUs shared between samples, the width at each end represents the percentage of reads of a certain MOTU in each sample; (5) grey connectors are the excluded ones when the network is thresholded; (6) coloured connectors are those remaining after thresholding

In each sample, an average of 1% of the reads (Table S1, Fig. S2) is clearly foreign to the community under study. These spurious reads probably originate by the stochastic presence of foreign fungal propagules, parasymbiotic stages of lichen forming fungi, spores or hyphae attached to or entangled within lichen thalli but do not have a stable ecological association with them as part of the lichen mycobiome. In fact, most spurious MOTUs blast to neighbouring lichen species (Fig. S2). These are easily excluded from the mycobiome data set but raised an intuitive expectation: if a second lichen fungus is found in a sample, due to spore dispersal or contamination, the species specific to its mycobiome may also be found with a similar probability in the sample. Despite of the inaccuracy of amplicon-based methods, we followed this rationale and used the identifiable spurious fraction to provide a confidence threshold of read coverage (percentage) below which MOTUs cannot be safely considered constitutive of a sample. More precisely, we identified in each sample spurious MOTUs when they blasted to (i) lichen mycobiont other than the mycobiont of that specific sample, (ii) taxa that are locally absent, that is, that are not part of the alpine lichen communities (i.e., Lobariaceae), (iii) other fungi which unlikely play a part in the lichenicolous community, such as wood decaying and mycorrhizal Basidiomycota. The threshold used was the average coverage of spurious MOTUs per sample (Table 1), and a minimum threshold of 0.01% was imposed for samples where no spurious reads were found. Threshold-filtered networks were therefore calculated after reducing the data set using the sample-specific thresholds.

Unipartite networks were described in terms of their connectance (Dunne, Williams, & Martinez, 2002) and the distribution of normalized paired differences index (PDI) (Poisot, Bever, Nemri, Thrall, & Hochberg, 2011) across samples. This gives an idea of the specialization in species interactions which can be interpreted as sample-specific proxy for a normalized measurement of interaction strength. Bipartite networks (Appendix S1) were numerically described using the wrapper function *networklevel* in terms of their connectance, compartmentalization (Tylianakis, Tscharntke, & Lewis, 2007) and nestedness (Almeida-Neto, Guimarães, Guimaraes, Loyola, & Ulrich, 2008; Galeano, Pastor, & Iriondo, 2009; Rodríguez-Gironés & Santamaría, 2006). Further network indices were also included to provide comparison with the bipartite networks calculated at species level (Table 3).

## 2.8 | Bipartite networks between lichen host species and MOTUs of the associated fungi

Bipartite interaction networks between host lichen species and MOTUs were generated from the MOTUs per sample table (Table 4) by pooling all samples of the same species and normalizing using species totals. As above, networks were obtained for the complete taxonomic set and for the four major fungal orders detected, both

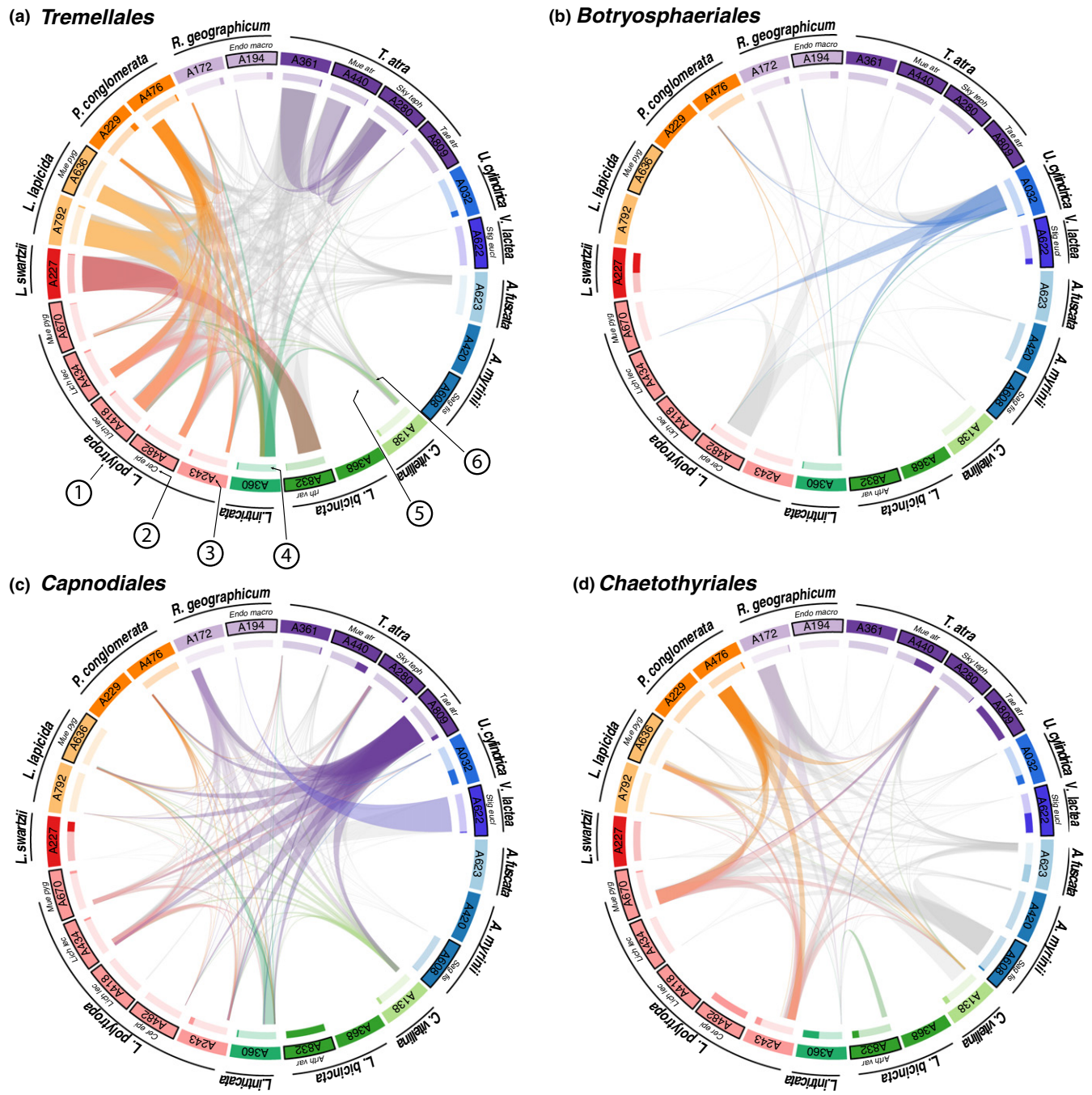


**FIGURE 4** Circos plot summarizing uni- and bipartite networks for the four focus orders: (a) Tremellales, (b) Botryosphaeriales, (c) Capnodiales and (d) Chaetothyriales. The meaning of the different elements of the plot corresponds to caption of Figure 3

unfiltered and filtered, using the sample-specific thresholds. Each network was numerically described (Table 3) using the wrapper function *networklevel* and visualized using *plotweb* and *visweb* functions (Appendix S1) all from R package BIPARTITE (Dormann et al., 2008, 2009). Species networks provide a more solid ecological perspective than sample networks, but their results may suffer from the unbalanced sampling design. They provide, however, a biological discussion that cannot be substituted by sample networks. As the overall topology was studied at sample level, we focused on studying each network in terms of compartmentalization (Tylianakis et al., 2007), connectance (Dunne et al., 2002; Tylianakis et al., 2007), weighted nestedness (Almeida-Neto et al., 2008; Galeano et al., 2009; Rodríguez-Gironés & Santamaría, 2006), web asymmetry (Blüthgen, Fründ, Vázquez, & Menzel, 2008; Blüthgen, Menzel, Hovestadt, Fiala, & Blüthgen, 2007), number of shared partners and niche overlap at higher and lower levels (Table 4). The contribution of each row and column to nestedness was calculated using function *nestedcontribution* run on 499 simulations. In addition to the described network

**TABLE 3** Numerical description of unipartite sample networks and bipartite networks at sample and host species levels. Networks are calculated for the complete data set, and for partial data sets using only MOTUs identified within Tremellales, Botryosphaeriales, Capnodiales and Chaetothyriales. Network metrics are calculated using the unfiltered raw data set (R) and imposing a sample-specific threshold based on the average proportion of spurious MOTU reads (Table 1). Using a threshold filtering consistently filters out singletons and low coverage MOTUs, simplifying the resulting networks. While unipartite sample networks always include the 25 samples considered, bipartite networks only consider the subset of samples in which usable reads are found, a number that may differ between threshold-filtered and unfiltered scenarios. A thorough numerical description is provided in the SM

| Samples | All | | Tremellales | | Botryosphaeriales | | Capnodiales | | Chaetothyriales | |
|---|---|---|---|---|---|---|---|---|---|---|
| **Unipartite networks** | **R** | **T** | **R** | **T** | **R** | **T** | **R** | **T** | **R** | **T** |
| Connectance (25*25) | 0.77 | 0.38 | 0.62 | 0.23 | 0.15 | 0.05 | 0.46 | 0.24 | 0.40 | 0.09 |
| Loss of connectance | | 0.39 | | 0.38 | | 0.10 | | 0.22 | | 0.31 |
| Number of links per sample | 9.68 | 4.42 | 7.10 | 2.34 | 1.13 | 0.23 | 4.61 | 1.89 | 4.2 | 0.43 |
| Mean number of common links | 15.92 | 4.94 | 11.28 | 2.13 | 1.06 | 0.21 | 7.18 | 2.53 | 5.32 | 0.50 |
| **Bipartite networks** | | | | | | | | | | |
| Number of MOTUs | 1396 | 138 | 219 | 24 | 90 | 10 | 292 | 22 | 154 | 29 |
| Number of samples | 25 | 24 | 23 | 20 | 15 | 9 | 21 | 17 | 23 | 12 |
| Mean shared MOTUs per pair of samples | 0.09 | 0.21 | 0.14 | 0.26 | 0.38 | 0.58 | 0.21 | 0.32 | 0.19 | 0.38 |
| Mean common samples per pair of MOTUs | 2.99 | 0.91 | 1.32 | 0.46 | 0.64 | 0.61 | 1.07 | 0.61 | 0.66 | 0.52 |
| Connectance | 0.05 | 0.07 | 0.06 | 0.11 | 0.09 | 0.24 | 0.06 | 0.11 | 0.06 | 0.13 |
| Number of compartments | 1 | 2 | 1 | 1 | 1 | 1 | 2 | 3 | 3 | 2 |
| Nestedness | 8.05 | 8.64 | 5.81 | 13.38 | 5.99 | 24.49 | 3.81 | 8.23 | 4.02 | 11.11 |
| Weighted nestedness | 0.43 | 0.38 | 0.59 | 0.53 | 0.79 | 0.34 | 0.74 | 0.64 | 0.63 | 0.53 |
| Weighted NODF | 1.92 | 8.16 | 3.89 | 13.50 | 6.66 | 17.90 | 2.87 | 15.87 | 5.71 | 13.91 |
| Cluster coefficient | 0.04 | 0.04 | 0.04 | 0.05 | 0.07 | 0.17 | 0.05 | 0.06 | 0.04 | 0.08 |
| Cluster coefficient MOTUs | 0.29 | 0.18 | 0.48 | 0.31 | 0.29 | 0.26 | 0.42 | 0.40 | 0.31 | 0.33 |
| Cluster coefficient sample | 0.05 | 0.07 | 0.09 | 0.13 | 0.35 | 0.41 | 0.17 | 0.17 | 0.10 | 0.15 |
| Weighted cluster coefficient MOTUs | 0.90 | 0.63 | 0.52 | 0.03 | 0.35 | 0.19 | 0.42 | 0.20 | 0.30 | 0.06 |
| Weighted cluster coefficient sample | 0.04 | 0.16 | 0.04 | 0.03 | 0.03 | 0.20 | 0.01 | 0.10 | 0.02 | 0.02 |
| C-score MOTUs | 0.92 | 0.82 | 0.86 | 0.80 | 0.62 | 0.59 | 0.79 | 0.72 | 0.82 | 0.65 |
| C-score sample | 0.87 | 0.80 | 0.66 | 0.67 | 0.70 | 0.57 | 0.58 | 0.52 | 0.73 | 0.66 |

| Species | All | | Tremellales | | Botryosphaeriales | | Capnodiales | | Chaetothyriales | |
|---|---|---|---|---|---|---|---|---|---|---|
| **Bipartite networks** | **R** | **T** | **R** | **T** | **R** | **T** | **R** | **T** | **R** | **T** |
| Number of MOTUs | 1396 | 166 | 219 | 30 | 90 | 9 | 292 | 30 | 154 | 26 |
| Number of host species | 13 | 12 | 13 | 9 | 10 | 6 | 12 | 9 | 13 | 9 |
| Connectance | 0.09 | 0.11 | 0.09 | 0.16 | 0.13 | 0.35 | 0.10 | 0.16 | 0.09 | 0.17 |
| Weighted connectance | 0.00 | 0.03 | 0.01 | 0.06 | 0.02 | 0.11 | 0.01 | 0.06 | 0.01 | 0.06 |
| Number of compartments | 1 | 1 | 1 | 1 | 1 | 1 | 2 | 2 | 1 | 1 |
| Nestedness | 12.68 | 9.12 | 10.21 | 13.46 | 12.03 | 17.32 | 8.99 | 13.55 | 9.79 | 13.86 |
| Weighted nestedness | 0.50 | 0.71 | 0.63 | 0.75 | 0.75 | 0.38 | 0.75 | 0.73 | 0.58 | 0.63 |
| Weighted NODF | 3.62 | 19.10 | 5.24 | 23.64 | 8.50 | 24.51 | 5.07 | 18.05 | 9.39 | 24.06 |
| Web asymmetry | 0.98 | 0.87 | 0.89 | 0.54 | 0.80 | 0.20 | 0.92 | 0.54 | 0.84 | 0.49 |
| Links per species | 1.12 | 1.26 | 1.12 | 1.08 | 1.15 | 1.27 | 1.10 | 1.08 | 1.14 | 1.11 |
| Cluster coefficient | 0.08 | 0.08 | 0.08 | 0.11 | 0.10 | 0.33 | 0.08 | 0.11 | 0.08 | 0.11 |
| Cluster coefficient MOTUs | 0.37 | 0.24 | 0.48 | 0.37 | 0.42 | 0.35 | 0.47 | 0.45 | 0.42 | 0.36 |

(Continues)

**TABLE 3** (Continued)

| Species | All | | Tremellales | | Botryosphaeriales | | Capnodiales | | Chaetothyriales | |
|---|---|---|---|---|---|---|---|---|---|---|
| Bipartite networks | R | T | R | T | R | T | R | T | R | T |
| Cluster coefficient host species | 0.13 | 0.22 | 0.18 | 0.22 | 0.37 | 0.56 | 0.25 | 0.22 | 0.16 | 0.26 |
| Weighted cluster coefficient MOTUs | 0.96 | 0.75 | 0.66 | 0.06 | 0.62 | 0.36 | 0.68 | 0.31 | 0.45 | 0.04 |
| Weighted cluster coefficient host species | 0.02 | 0.07 | 0.02 | 0.01 | 0.05 | 0.16 | 0.02 | 0.05 | 0.03 | 0.02 |
| C-score MOTUs | 0.82 | 0.39 | 0.78 | 0.38 | 0.60 | 0.32 | 0.67 | 0.50 | 0.67 | 0.22 |
| C-score host species | 0.86 | 0.73 | 0.73 | 0.60 | 0.60 | 0.39 | 0.59 | 0.43 | 0.73 | 0.60 |

metrics, we included additional summary metrics in the tables to give a more thorough description of the data set and to enable detailed critical reading of this study.

### 2.9 | Specificity of lichen hosts towards lichenicolous fungi and their mycobiomes

The degree of specificity of lichen hosts towards their mycobiomes was estimated on bipartite networks using the standardized specialization index (d') proposed by Blüthgen, Menzel, and Blüthgen (2006) as implemented in function *dfun* of R package BIPARTITE. Specificity was also assessed for MOTUs identifiable as lichenicolous fungi towards their hosts (Table 2), and vice versa. For every case, specialization was estimated both in unfiltered and in threshold-filtered networks. Graphic representations of the networks can be found in Figure 3, and specialization estimates are summarized in Table 5.

### 2.10 | Clustering and mycobiome structure

To test whether the samples collected represented subsets of a single species (MOTU) pool (meta-mycobiome) or reflected the presence of different lichen mycobiomes, we carried out Gaussian finite mixture clustering using the EM algorithm implemented in function *mclust* of the homonymous R package (Fraley & Raftery, 2002; Fraley et al., 2012). A simple hierarchical clustering approach on a Bray–Curtis dissimilarity matrix calculated from the MOTU table was also performed for graphical purposes. For this, we used the functions *vegdist* from package VEGAN and HCLUST from the base R package. Additionally, the presence of multiple MOTU pools was tested using a k- medioids clustering on a covariance matrix of MOTU occurrences per sample. For the covariance matrix, we used R function *cov* included in the BASE package, and to estimate the optimum number of clusters, we used an optimum silhouette width criterion as implemented in function *pamk* of package FPC (Henning, 2015). The assignment to the main taxonomic categories is summarized in Figure 2 and is further detailed in Appendix S1.

### 2.11 | Estimation of $\alpha$- and $\beta$-diversity

Rarefaction curves of MOTU richness and taxonomic richness per read were elaborated using a recursive implementation of function *rarefy* of R package VEGAN (Oksanen, 2015; Oksanen et al., 2015) and are reported in Appendix S1. Rarefaction was carried out in data sets of reads per MOTU and reads per taxonomic group, respectively. The comparison of $\alpha$-diversities between infected and noninfected samples was carried out using a z-statistic on the average richness and standard deviations of samples belonging to each category per each step of rarefied sequencing depth. It should be noted that due to the uneven number of reads per sample, there is a progressive loss of replication across the comparisons as rarefaction factor increases. Estimators of MOTU richness based on species accumulation models (chao1 and jackknifed) were calculated using functions *estimateR* and *specpool* for each sample and for the complete data-set. Beta diversity between samples was calculated using R package VEGAN using function *betadiv*. An estimate of multivariate dispersions comparing infected and noninfected samples was obtained with function *vegdist*. The analyses were carried out both including and excluding singletons.

## 3 | RESULTS

The 454-pyrosequencing run generated 399.593 reads of an average length of ca. 400 bp, and a median of 33 for the quality phred-score averaged per sequence. Being relatively high, it does not account for the homopolymer bias typical of the sequencing platform. A detailed quality report on the raw output files is included in the Supplementary material (Appendix S1, Fig. S55). Despite the careful equimolar pooling of sequencing libraries, the sequencing depths of the 26 samples were heterogeneous with read numbers ranging between 936 and 8750 per sample (Table 2). This is probably due to significant differences in amplicon size distribution between samples, coherent with the uneven presence of group I introns at the end of SSU. Sample A405 contained only sequences of the lichen mycobiont (Table 1, Table S1, Fig. S1) with the exception of two unidentified ITS1 amplicons and was therefore excluded from further analyses.

### 3.1 | Identifying lichen mycobionts

The proportion of reads identified to belong to the sample's mycobiont is quite uneven. On average, it represents 56% of the reads per sample, but it ranges between 3.5% and 97.7% (SF2, Tables 1 and 2). Notwithstanding this disparity, we observed that in general

**TABLE 4** Discrepancy between the number of exclusive and shared MOTUs per sample and the number of reads they comprise. The table reports the number of MOTUs that are exclusive to each sample and the number of MOTUs that are shared with any other sample in the data set, as well as the total number of reads that represent shared and exclusive MOTUs. The data are given for the whole data set as well as for the four most abundant fungal orders Botryosphaeriales, Capnodiales, Chaetothyriales and Tremellales

| | Tremellales | | | | Capnodiales | | | | Chaetothyriales | | | | Botryosphaeriales | | | | Total | | | |
|---|---|---|---|---|---|---|---|---|---|---|---|---|---|---|---|---|---|---|---|---|
| | OTUs | | Reads | | OTUs | | Reads | | OTUs | | Reads | | OTUs | | Reads | | OTUs | | Reads | |
| | Shared | Exclusive | Shared | Exclusive | Shared | Exclusive | Shared | Exclusive | Shared | Exclusive | Shared | Exclusive | Shared | Exclusive | Shared | Exclusive | Shared | Exclusive | Shared | Exclusive |
| Aca_fus+N+A623 | 3 | | 5 | | | | | | 3 | 2 | 5 | 4 | | | | | 7 | 6 | 11 | 8 |
| Aspi_myr+N+A420 | | | | | | | | | 1 | | 2 | | 1 | | 1 | | 3 | 1 | 34 | 1 |
| Can_vit+N+A138 | 5 | 2 | 35 | 2 | 2 | 2 | 27 | 2 | 4 | 11 | 90 | 13 | 2 | | 4 | | 13 | 19 | 156 | 21 |
| Leca_bic+N+A368 | | | | | | | | | | | | | | | | | 1 | 1 | 15 | 1 |
| Leca_intr+N+A360 | 4 | 32 | 2241 | 69 | 10 | 43 | 1836 | 64 | 4 | 9 | 45 | 31 | 5 | 6 | 413 | 9 | 30 | 135 | 4980 | 242 |
| Leca_poly+N+A243 | 5 | 14 | 286 | 18 | 8 | 6 | 171 | 22 | 9 | 38 | 955 | 170 | 1 | | 2 | | 36 | 87 | 2218 | 322 |
| Leca_schw+N+A227 | 5 | 26 | 6122 | 42 | 2 | 1 | 3 | 1 | 2 | | 10 | | 1 | 1 | 1 | 1 | 14 | 51 | 6157 | 70 |
| Leci_lap+N+A792 | 5 | 30 | 799 | 36 | 3 | | 6 | | 5 | | 20 | | | | | | 22 | 47 | 846 | 53 |
| Psori_con+N+A229 | 2 | 1 | 6 | 1 | | | | | 1 | | 1 | | | | | | 6 | 8 | 45 | 8 |
| Psori_con+N+A476 | 2 | 7 | 198 | 7 | 3 | | 27 | | 2 | 8 | 216 | 8 | 2 | | 21 | | 13 | 15 | 467 | 15 |
| Rhi_geo+N+A172 | 1 | 1 | 10 | 1 | 1 | | 44 | | 1 | 3 | 91 | 3 | 1 | 2 | 21 | 3 | 4 | 7 | 166 | 8 |
| Teph_atr+N+A361 | 9 | 24 | 6068 | 27 | 7 | 3 | 118 | 3 | 1 | | 1 | | 3 | | 12 | | 23 | 58 | 6203 | 61 |
| Umb_cyl+N+A032 | 1 | 1 | 6 | 1 | 4 | 14 | 105 | 64 | 4 | 7 | 38 | 11 | 4 | 42 | 2015 | 48 | 17 | 122 | 2194 | 550 |
| Aspi_myr+Sag_fis+A608 | 1 | | 22 | | 1 | | 2 | | 2 | 8 | 859 | 37 | | | | | 8 | 27 | 1030 | 63 |
| Leca_bic+Arth_var+A832 | 2 | 1 | 179 | 1 | | 7 | | 25 | 1 | 3 | 40 | 8 | | | | | 6 | 16 | 234 | 40 |
| Leca_poly+Cer_epi+A482 | 4 | 11 | 298 | 13 | 1 | | 13 | | | 1 | | 1 | 3 | | 1000 | | 9 | 19 | 1312 | 21 |
| Leca_poly+Lich_lec+A418 | 2 | 1 | 28 | 1 | 1 | | 2 | | | | | | | | | | 5 | 3 | 49 | 3 |
| Leca_poly+Lich_lec+A434 | 6 | 11 | 271 | 11 | 3 | 10 | 198 | 10 | 1 | | 4 | | | | | | 17 | 41 | 869 | 60 |
| Leca_poly+Mue_pyg+A670 | 4 | 4 | 233 | 4 | 4 | 4 | 355 | 24 | 6 | 28 | 1139 | 39 | 2 | | 9 | | 22 | 74 | 2478 | 110 |
| Leci_lap+Mue_pyg+A636 | 2 | | 40 | | 2 | | 6 | | 5 | | 21 | | | | | | 14 | 1 | 80 | 1 |
| Rhi_geo+Endo_macro+A194 | 4 | 3 | 17 | 3 | 2 | | 11 | | 1 | | 1 | | 4 | 2 | 36 | 9 | 12 | 42 | 996 | 112 |
| Teph_atr+Mue_atr+A440 | 6 | 6 | 743 | 9 | 6 | 4 | 56 | 24 | 1 | 2 | 2 | 2 | 2 | | 4 | | 17 | 49 | 988 | 82 |
| Teph_atr+Sky_teph+A280 | 9 | 26 | 3495 | 43 | 8 | 29 | 749 | 36 | 5 | 13 | 885 | 14 | 3 | 1 | 29 | 1 | 34 | 118 | 5730 | 158 |
| Teph_atr+Tae_atr+A809 | 6 | | 89 | | 3 | 92 | 4727 | 498 | | 1 | | 2 | | | | | 9 | 100 | 4816 | 514 |
| Vari_lac+Stig_eucl+A622 | 3 | | 10 | | 6 | 57 | 2835 | 72 | 2 | 3 | 3 | 3 | 1 | 2 | 12 | 2 | 14 | 73 | 2863 | 89 |

**TABLE 5** Standardized and raw specialization indices calculated for each lichen host species (A) in the networks, as well as for those lichenicolous fungi identifiable as the main MOTUs at sample level (B). The values of d' (highlighted in bold) range between 0 = no specialization and 1 = perfect specialization

| | All OTUs | | | | | | | | Main Lichenicolous fungi MOTUs only | | | | | | | |
|---|---|---|---|---|---|---|---|---|---|---|---|---|---|---|---|---|
| | Complete | | | | Threshold filtered | | | | Complete | | | | Threshold filtered | | | |
| | d' | d | dmin | dmax | d' | d | dmin | dmax | d' | d | dmin | dmax | d' | d | dmin | dmax |
| (A) | | | | | | | | | | | | | | | | |
| *Acarospora fuscata* | **0.39** | 2.54 | 2.12 | 3.22 | | | | 3 | | | | | | | | |
| *Aspilidea myrinii* | **0.97** | 2.50 | 1.73 | 2.53 | **0.99** | 2.68 | 2.02 | 2.69 | **0.97** | 2.26 | 1.52 | 2.28 | **0.99** | 2.27 | 1.52 | 2.27 |
| *Candelariella vitellina* | **0.00** | 2.08 | 2.08 | 3.22 | **0.33** | 2.48 | 2.03 | 3.40 | **0.00** | 0.83 | 0.83 | 3.52 | **0.00** | 1.00 | 1.00 | 3.59 |
| *Lecanora bicincta* | **0.60** | 2.20 | 1.73 | 2.53 | **0.29** | 2.17 | 2.03 | 2.51 | . | . | . | . | . | . | . | . |
| *Lecanora intricata* | **0.00** | 2.03 | 2.03 | 3.22 | **0.00** | 1.94 | 1.94 | 3.13 | **0.00** | 1.32 | 1.32 | 4.15 | **0.00** | 1.33 | 1.33 | 4.14 |
| *Lecanora polytropa* | **0.00** | 1.02 | 1.02 | 1.61 | **0.00** | 0.96 | 0.96 | 1.50 | **0.00** | 0.79 | 0.79 | 1.19 | **0.00** | 0.79 | 0.79 | 1.19 |
| *Lecanora swartzii* | **0.51** | 2.68 | 2.12 | 3.22 | **0.52** | 2.59 | 2.03 | 3.11 | **0.00** | 1.09 | 1.09 | 8.23 | | | | |
| *Lecidea lapicida* | **0.00** | 1.50 | 1.50 | 2.53 | **0.00** | 1.44 | 1.44 | 2.44 | **0.00** | 1.06 | 1.06 | 3.56 | **0.00** | 1.08 | 1.08 | 3.56 |
| *Psorinia conglomerata* | **0.00** | 1.66 | 1.66 | 2.53 | **0.00** | 1.64 | 1.64 | 2.53 | **0.00** | 1.23 | 1.23 | 2.60 | **0.00** | 1.37 | 1.37 | 2.64 |
| *Rhizocarpon geographicum* | **0.33** | 1.99 | 1.73 | 2.53 | **0.00** | 2.00 | 2.00 | 2.47 | **0.00** | 1.41 | 1.41 | 1.88 | **0.00** | 1.46 | 1.46 | 1.88 |
| *Tephromela atra* | **0.48** | 1.53 | 1.25 | 1.83 | **0.46** | 1.52 | 1.32 | 1.75 | **0.00** | 1.36 | 1.36 | 1.83 | **0.00** | 1.36 | 1.36 | 1.82 |
| *Umbilicaria cylindrica* | **0.78** | 2.97 | 2.12 | 3.22 | **0.85** | 3.08 | 2.03 | 3.26 | **0.02** | 1.71 | 1.52 | 9.20 | | | | |
| *Varicellaria lactea* | **0.94** | 3.15 | 2.12 | 3.22 | **0.99** | 3.12 | 2.03 | 3.13 | **0.95** | 1.99 | 1.52 | 2.02 | **1.00** | 2.01 | 1.52 | 2.01 |
| (B) | | | | | | | | | | | | | | | | |
| *Muellerella pygmaea 21* | | | | | | | | | **0.00** | 0.93 | 0.93 | 1.71 | **0.00** | 0.94 | 0.94 | 1.70 |
| *Sagediopsis fissurisedens 34* | | | | | | | | | **0.96** | 2.23 | 1.19 | 2.27 | **0.96** | 2.23 | 1.19 | 2.27 |
| *Cercidospora epipolytropa 18* | | | | | | | | | **0.00** | 1.13 | 1.13 | 2.28 | **0.00** | 1.19 | 1.19 | 2.30 |
| *Lichenoconium lecanorae 32* | | | | | | | | | **0.00** | 1.14 | 1.14 | 2.21 | **0.00** | 1.15 | 1.15 | 2.20 |
| *Endococcus macrosporus 17* | | | | | | | | | **0.64** | 1.79 | 1.19 | 2.13 | **0.73** | 1.88 | 1.19 | 2.14 |
| *Muellerella atricola 46* | | | | | | | | | **0.24** | 1.81 | 1.19 | 3.75 | **0.25** | 1.82 | 1.19 | 3.75 |
| *Skyttea tephromelarum 33* | | | | | | | | | **0.17** | 1.77 | 1.19 | 4.63 | **0.18** | 1.82 | 1.19 | 4.63 |
| *Taeniolella atricerebrina 10* | | | | | | | | | **0.00** | 0.74 | 0.74 | 1.52 | **0.00** | 0.75 | 0.75 | 1.52 |
| *Stigmidium eucline 12* | | | | | | | | | **0.93** | 1.96 | 1.19 | 2.01 | **1.00** | 2.01 | 1.19 | 2.01 |

the most abundant MOTUs were identified to belong to the mycobiont and the symptomatic lichenicolous fungus when present (Table 2), which together represent an average of 63% of the reads per sample. In twelve samples, the mycobiont sequences did not contain an usable ITS1 fraction.

Before filtering for ITS1, an average of 1.2% of the sample reads, ranging between 0% and 9% (SF1) in individual samples, represented fungal taxa foreign to the focal community. These reads blasted to lichen fungi other than the mycobiont of the sample, as well as to fungi which are unlikely to play a part in the lichen-associated community, as wood decaying and obligate mycorrhizal Basidiomycota.

Most spurious reads identified as foreign mycobionts corresponded to species and MOTUs found in the local community under study. These were consistently filtered out of the data set for mycobiome analyses (Table 1, Table S1, Fig. S2). However, we also identified locally absent, nonlichenicolous mycobionts (i.e., Lobariaceae but not Micareaceae, a family that contains lichenicolous lichens). Because we do not have any explanation on why they may be present and constitute a low fraction of the overall sample data set, we did not filter them out of the data set. The extent to which the unfiltered data set may be composed of lichen mycobionts cannot be soundly ascertained, as intronic sequences render many taxonomic placements unreliable; for example, Lecanoromycetes tend to blast to *Umbilicaria* sp., a lichen genus highly represented in the NCBI database (SF3-SF8).

## 3.2 | Identifying symptomatic lichenicolous fungi

The MOTUs identified as those corresponding to the lichenicolous fungus for each sample can be found in Table 2. All infected samples but one (A832) contained a major MOTU clearly belonging to the lichenicolous fungus (Table 2). However, reference sequences in NCBI are available only for *Endococcus fusigera* (FJ645262), *Taeniolella stilbospora* (AY843127), *Skyttea gregaria* (KJ559537), *S. radiatilis* (KJ559536, KJ559538) and *S. tephromelarum* (Sk145, A. Suija, unpublished). Most sequences belonging to lichenicolous fungi should be therefore interpreted indirectly from sequencing depth and taxonomic assignment. Sample A832 of *Lecanora bicincta*

rendered no sequences that could be either identified or interpreted as the occurring lichenicolous fungus *Arthonia varians*, suggesting that divergent lineages of Ascomycota such as Arthoniaceae may be underrepresented due to low affinity to the primers used.

*Endococcus macrosporus* is identified as MOTU 17, found symptomatic in sample A194, and asymptomatic in A229 and A360. The ITS1 sequences render no significant taxonomic assignment, but the untrimmed sequence clusters blasted mainly to *Bagliettoa marmorea* (Verrucariaceae). The reference sequence of MOTU 17 is 69% identical to the *E. fusigera* reference (FJ645262) and 68% identical to an ITS sequence obtained from a cultured strain (A889) originating from the same sample A194.

In sample A809 *Tephromela atra*, MOTU 10 is the most likely to be the infecting *Taeniolella atricerebrina*, blasting to closely related taxa in the Mycosphaerellaceae (Dothideomycetes, SF16). However, MOTUs identified as *Taeniolella* (MOTU 141, 196, 1291, 1393) are present also in other samples of *Tephromela atra* (A361 and A440) devoid of *Taeniolella atricerebrina* infection and in additional three lichens other than *Tephromela atra* (samples A243, A476, A172). These MOTUs are on average 70% similar to the ITS1 sequence of *Taeniolella stilbospora* (AY843127) available in GenBank.

In the sample of *Tephromela atra* (A280) infected by *Skyttea tephromelarum*, the 411 reads of MOTU 33 blasted with *Skyttea* species available in GenBank (*S. gregaria* KJ559537; *S. radiatilis* KJ559536, KJ559538) and with a sequence of *Skyttea tephromelarum* Sk145 unpublished (kindly provided by A. Sujia; SF16). MOTU 33 s therefore interpreted to be the occurring lichenicolous fungus *Skyttea tephromelarum*.

*Muellerella pygmaea* infecting samples of *Lecanora polytropa* (A670) and *Lecidea lapicida* (A636) likely correspond to MOTU 21, which is common to both. The *M. pygmaea* infecting *Rhizocarpon geographicum* was expected to be divergent from the rest based on microscopical observations (ascospore size), and while it was probably captured in a sequence cluster, it was not found in the ITS1 data set.

We had no reference sequences to compare the identities of MOTU 34 (*Sagediopsis fissurisedens*), MOTU 18 (*Cercidospora epipolytropa*), MOTU 32 (*Lichenoconium lecanorae*), MOTU 46 (*Muellerella atricola*) and MOTU 12 (*Stigmidium eucline*).

## 3.3 | Taxonomic structure of the lichen mycobiomes

The results of the taxonomic assignment of MOTUs are summarized in Figure 2 and at different taxonomic depths in the supplementary material (Tables S3 and S4; Figs S3–S7).

After taxonomic assignment, before and after trimming the ITS1 and lichen sequences, Ascomycota and Basidiomycota fungi are represented evenly in the data set. About 4% of the trimmed data set was not identifiable at division level; the unidentifiable proportion rises up to 24% in the untrimmed data set due to the presence of group I intronic sequences (Figure 2), despite of having used the broader NCBI database for identification. The proportion of reads assigned to Ascomycota and Basidiomycota differs strongly between samples. A single read was identified as Chytridiomycota.

Most reads are identified as Ascomycota in 15 of the 26 samples. At class level, the most represented Ascomycota belong to Dothideomycetes in 11 samples, to Eurotiomycetes in 12 samples and to a lesser extent to Lecanoromycetes (2 samples). Leotiomycetes are only marginally relevant in the single sample of *Umbilicaria cylindrica* (A032). At order level, the most abundant were Chaetothyriales, Capnodiales and Botryosphaeriales, found in 23, 21 and 15 samples, respectively. Additionally, Pleosporales, Lecanorales, Myriangiales, Helotiales and Hypocreales were found in 11, 11, 8, 6, 3 samples, respectively (SF6). The MOTUs blasting in Dothideomycetes mainly represented the families Teratosphaeriaceae, Mycosphaerellaceae and Myriangiaceae; those blasting in Chaetothyriales mainly represented the family Herpotrichiellaceae (Table S2, Figs S3 and S7).

Reads identified as Basidiomycota are not found in three samples, whereas they are consistently found in all the remaining samples and are the main component of 11 of them. Most reads of Basidiomycota blast to 25 MOTUs of Tremellomycetes, matching reference sequences of Sirobasidiaceae (Tremellomycetes, Tremellales), in particular to the genus *Fibulobasidium*. Some reads blasting to Russulales, Agaricales and Polyporales represent very small proportions of the samples in which they are found (Table S3; Figs S3–S7).

## 3.4 | Clustering of the MOTU community table

Using model-based clustering (Gaussian finite mixture model implemented in *mclust*) on the normalized matrix of reads per sample and excluding singletons, we estimated a diagonal multivariate normal model with a single component to be the best model (25 samples, 520 degrees of freedom, log likelihood of −13673.21, BIC of −29020.23 and ICL of −29020.23). Using k-medioids clustering on a covariance table between nonsingle MOTUs, we inferred the best model with three components. The first two components include each an abundant MOTU of Tremellales as single component, the third component grouped all remaining MOTUs.

## 3.5 | Shared and exclusive MOTUs and reads

There is a widespread discrepancy between the number of shared and exclusive MOTUs for each sample and the number of reads they represent (Table 4). This numerical displacement is caused by two factors: *i)* the number of exclusive MOTUs is overestimated due to the abundance of low coverage MOTUs, especially singletons, *ii)* the most abundant MOTUs are widely present across samples (Figure 3).

## 3.6 | Uni- and bipartite sample networks

A complete graphical representation of the sample networks is reported in the Supplementary Material (SF 18–33), while the overall topologies are summarized from the networks of Figures 3 and 4.

The communities of lichen-associated fungi form high-degree unipartite and bipartite sample-level networks, in accordance with the number of shared reads and MOTUs (Table 4). The unipartite sample network (Figure 3) has a very high connectance, including 77% of all possible links between samples. On average, each sample is connected with 16 other samples. However, when the data set is filtered using the sample-specific coverage thresholds (Table 1), this proportion decreases to 38% and the average number of connections per sample decreases to 4.94. This suggests that the widespread occurrence of spurious MOTUs has a significant impact on the network connectance. The bipartite sample networks have low connectance, even after the application of the sample thresholds, due to the numerical displacement between MOTU and sample levels (Table 3). The average number of shared MOTUs per sample decreases from three to 0.91 when the data set is threshold-filtered, emphasizing again the effect of spurious MOTUs on the interpretation of the data set. Both sample networks are noncompartmented and strongly nested, independently of whether weighted or unweighted estimators are used (Table 3).

The partial unipartite and bipartite networks focused in MOTUs belonging to the four most abundant fungal orders (Figure 4) show patterns similar to the complete networks (Figure 3, Table 3) with regard to the connectance and the effect of threshold filtering.

MOTUs of Tremellales are highly represented in the data set (Figures 2 and 4a). The Tremellales partial unipartite network (Figure 4a) shows the highest connectance, with 62% of the links present. The mean number of links per sample is 11.28; however, it decreases to 2.13 when filtering the data set, in accordance with the lower connectance (23%), as it results from the widespread presence of few MOTUs. The least connected network of Botryosphaeriales (Figure 4b), which are found in fewer samples (15), and Chaetothyriales (Figure 4d) drop from 15% to 5% connectance and from 40% to 9% when filtered, respectively. Capnodiales (Figure 4c) show a similarly connected graph (46%), but its links are more resilient to thresholding (24%). The partial networks show in all cases higher compartmentalization and slightly lower nestedness than the complete networks (Figure 3).

The bipartite network of Tremellales (Figure 4a) shows no compartmentalization and a high nestedness that diffuses when using a weighted estimator. Compartmentalization and nestedness are not significantly lost when the data set is filtered, as fewer samples are included in the network. Botryosphaeriales (Figure 4b) shows a contrasting pattern, with a low connectance network with fewer MOTUs and fewer samples. Although nestedness estimates on the whole network are similar to those of other orders, the application of the thresholds reduces the number of samples and of MOTUs to nine and ten, respectively; still, the network does not show a nested structure. The bipartite network of Capnodiales (Figure 4c) is compartmented, separating sample A832 of *L. bicincta* which has a large proportion of low coverage MOTUs, from the rest. After the application of the thresholds, the compartmentalization increases excluding A832 and separating from a main compartment linked by the widespread presence of MOTU 12, samples A418 in a single compartment and samples A194 and A622, linked by MOTU 10. Chaetothyriales (Figure 4d) also form a compartmented network with a major compartment and two single samples (A482 and A809). When thresholded, only the main compartment remains and samples of *A. myrinii* linked by the presence of MOTU 34 form a separate compartment. The networks of both Capnodiales and Chaetothyriales are highly nested when unfiltered and less nested when thresholded; though in Chaetothyriales, these estimates are not comparable as the thresholding reduces the number of samples from 23 to 14.

## 3.7 | Bipartite species networks and specialization

Bipartite interaction networks were calculated for the complete data set and for the four focus orders using host lichen species as units (SF22–55). All networks have low connectance, due to the presence of few host species and many MOTUs of lichen-associated fungi, even after threshold filtering. The connectance increases between raw and thresholded networks as observed in the sample networks, reflecting the lower number of hosts included in both networks (Table 3). Bipartite species networks are mostly noncompartmentalized, with the exception of Capnodiales where two compartments are found. Species networks are more nested using weighted and unweighted nestedness estimates than the sample networks; in the latter, the structure is inflated by the pseudoreplication introduced by accounting multiple times for taxon-specific MOTUs.

Most lichen hosts show low to intermediate specificity towards their mycobiomes, with an average standardized specialization index (d') of 0.38 (Table 5). The exceptions are *U. cylindrica*, *A. myrinii* and *V. lactea*, which are highly specific even in the case when the data set is threshold-filtered. A similar pattern can be observed when addressing the specialization of the targeted MOTUs of lichenicolous fungi, six of which are widespread and three occur specifically in few species; this pattern is only slightly strengthened by thresholding (Table 5). Crossing both trophic levels, we observe that highly specific species correspond to the pairs: *A. myrinii* and *S. fissurisedens* (MOTU 34) found symptomatic in A608 and asymptomatic in A420 and of *V. lactea* and *S. eucline* (MOTU 12) a pair found only in sample A622. Finally, *U. cylindrica* comprises a distinct mycobiome (Figs S3–S7, Tables S2 and S3) coherent with its different growth form (foliose). *E. macrosporus* (MOTU 17) is rarely found outside of *R. geographicum*.

## 3.8 | Trends in diversity and richness between infected and uninfected samples

The comparison of rarefied MOTU alpha diversities between infected and noninfected thalli is represented in Figure 5. In all cases, either including or excluding singletons, differences in rarefied $\alpha$-diversity are only significant using a higher number of read threshold and keeping the number of samples low. Otherwise, at intermediate levels of sampling intensity, differences are either insignificant or showing a slightly higher diversity of noninfected samples. The $\beta$-

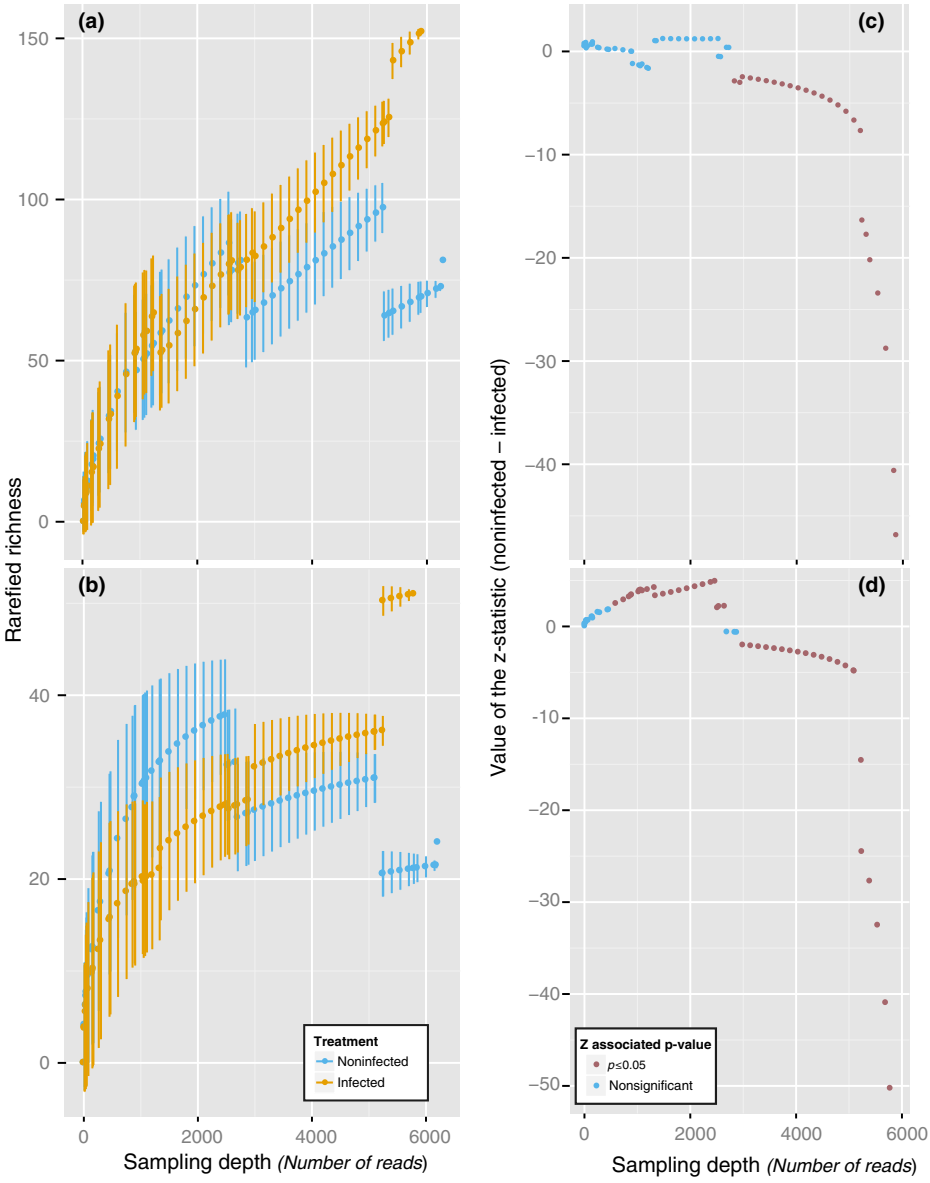


**FIGURE 5** Comparison of rarefied α-diversities between infected (orange) and noninfected (blue) samples. (a, b) Average MOTU richness and 95% confidence intervals (based on rarefied standard deviations per sample) per rarefaction intensity (number of sequences used). Variations in richness estimates reflect the different sample size used for each step of the simulation and are due to uneven sequencing depths and read numbers. (c, d) *Z*-value of the pairwise comparison of average rarefied MOTU richness. Red squares highlight statistical significance. Data sets used for simulations in (a) and (c) include singletons, those used in (b) and (d) excludes singletons (extended results are reported in Appendix S1)

diversity clustering analysis comparing infected and noninfected samples showed an equally inconclusive result (SF10-15) in which both treatments do not form identifiable clusters in the ordination. Pairwise β-diversities are stochastically distributed across samples and are not correlated with the lichen species host.

## 4 | DISCUSSION

The pervasive idea that lichens are phenotypically coherent associations formed by two symbiotic partners (i.e., one fungus and one alga) offers an overly simplified view on the biotic structure and function of lichen symbioses. In fact, lichens form complex symbiotic systems (Farrar, 1976) which include multiple photobiont lineages (del Campo et al., 2010, 2013; Casano et al., 2011; Muggia, Perez-Ortega, Kopun, Zellnig, & Grube, 2014; Piercey-Normore & Depriest, 2001; Stenroos et al., 2003; Wedin et al., 2015), highly specialized lichenicolous fungi (Lawrey & Diederich, 2003) and harbour complex communities of bacteria (Grube et al., 2009, 2015; Hodkinson & Lutzoni, 2010; Printzen, Fernández-Mendoza, Muggia, Grube, & Berg, 2012) and additional fungi (Arnold et al., 2009; Muggia et al., 2016; Spribille et al., 2016; Zhang et al., 2015). All together, these organisms are likely to contribute to the ecological characteristics and ultimate the evolutionary potential of the symbiotic system as a whole.

### 4.1 | Diversity and specificity of the lichen mycobiome

The lack of specificity of the fungi associated with different lichen hosts emerges as the main result of our study. The most abundant MOTUs, belonging to Tremellales, Capnodiales, Chaetothyriales and Botryosphaeriales, are consistently shared across samples and among lichen species (Table 4, Figures 3 and 4). These four orders contain most reads of the data set; together they account for 79% of the

ITS1 data set and a 36% of the unfiltered data set, which in turn contains a 23% of unidentified sequences vs. the 6.6% of the ITS1 data set. The fact that most known lichenicolous species (Lawrey & Diederich, 2017; Prillinger et al., 1997) also belongs in these orders suggests that many unidentified MOTUs may reflect the presence of asymptomatic lichenicolous fungi other than those targeted in our survey.

The lack of specificity to the lichen mycobiome is further supported by the lack of community structure observed using clustering and ordination methods (SF8 and SF9). This might be explained by the fact that many of the identified fungal MOTUs can represent parasymbiontic or commensal fungi and may show different trophic patterns along their life cycles, occurring only by chance in the lichen thalli. Furthermore, the low compartmentalization and the high nestedness estimated for all bipartite networks (Table 3, Figure 4, Table S4), as well as the low specificity of most samples towards their mycobiome (Table 5), suggest that the communities encountered across samples largely result from the subsampling of a shared "species pool". As an exception, *A. myrinii* and *V. lactea* have highly divergent mycobiomes, which are poor in MOTUs (Table 1, Tables S2 and S3, Figs S10–S15) and mostly composed of very specialized lichenicolous fungi (Table 5). Finally, the umbilicate lichen *U. cylindrica* also shows a divergent mycobiome, but this is not driven apart by a known lichenicolous component. Being *U. cylindrica* the only foliose species, it seems reasonable to propose that different anatomical heterogeneities and growth forms may provide diverse (micro)niches for lichen-associated organisms and hence adhere to divergent mycobiomes. This hypothesis, however, still need support by more detailed, forthcoming researches.

The presence of such spurious taxa reflects the functional and anatomical openness of lichen systems, which have rough and cracked outer surfaces and complex internal three-dimensional hyphal matrices that provide spaces in which spores, propagules, germinating hyphae, microscopic mycelia or even minute propagules of other fungi may remain attached. The pervasive presence of spurious reads challenges the interpretability of the observed mycobiome patterns and highlights the difficulty to filter out noise from signal in high-throughput sequencing experiments. Considering that spurious reads of identifiable components of the local mycota are often retrieved from lichen samples, it is quite intuitive to assume that our data set also comprises spurious reads of locally present lichen-associated fungi. Disregarding the systematic biases known to hamper the quantitative interpretation of amplicon-based studies (Amend, Seifert, & Bruns, 2010), we could expect them to be present in similar amounts. Such fungal reads would blur the structure of the lichen mycobiome, overestimating sample diversity and connectance of the community network across species and samples.

Threshold filtering of the data set had an important effect on the numeric outcome of the network structure and its associated metrics, always tending to reflect slightly less nested, more substructured networks (Table S4). Regardless of whether threshold filtering was implemented or not, the overall patterns of connectance, nestedness and specificity are highly coherent with each other (Table 3, Tables S4 and S5). We observe that the lack of host specificity of the mycobiome is coherent with previous results based on cultured strains isolated from the interior of surface-sterilized lichen thalli (Arnold et al., 2009; U'Ren et al., 2010, 2012). However, our data set is significantly poorer in endolichenic/endophytic Sordariomycetes, Pezizomycetes and Leotiomycetes than those obtained using culture-based experiments (Arnold et al., 2009; Muggia et al., 2016; U'Ren et al., 2010, 2012). The taxonomic divergence between culture-based and amplicon-based surveys was already encountered and thoroughly discussed by U'Ren et al. (2014) as a result of using only the culturable fraction, as well as primer bias.

## 4.2 | Lichenicolous fungi are widely found asymptomatic

Introducing symptomatically infected thalli into our methodological design allowed us to test the extent to which the sequenced mycobiome included aforeknown lichenicolous fungi and the extent to which the mycobiome may change in diversity as a result of a fungal infection. To date, in fact, the surveys dealing with lichen-associated fungal communities and applying the most up-to-date approaches for their analysis have neither included thalli with obvious symptoms of infection, nor regarded the previous knowledge on lichenicolous fungi. Also, they have mostly been based on studying the taxonomic fraction isolated using axenic culture methods, therefore omitting those highly specialized, host-specific taxa which have ecological requirements that are difficult to simulate in vitro or remain simply unknown. Past methodological choices led to the identification of a pool of unspecific asymptomatic, parasymbiotic or commensal fungi within lichen thalli, for which the concept of endolichenic fungi was coined (Arnold et al., 2009).

We observe that an important fraction of the fungal sequences retrieved from infected and uninfected lichen thalli belong to the lichenicolous fungi identified by morphology in the infected samples (Table 2, Figure 3). Apart from being identified as major components of the mycobiome in the symptomatically infected lichen samples, lichenicolous fungi are found asymptomatic in thalli of their typical hosts, sometimes with a high number of reads. Moreover, we found that six of the nine lichenicolous MOTUs identified in the infected samples are found widespread across the data set (Fig. S3, Table S5) and their presence lies often above the threshold criterium implemented in the study. These six MOTUs show no specificity towards their hosts, identified using the standardized specialization index (d') on bipartite species networks (Table 5). *Endococcus macrosporus* (MOTU 17) found in *R. geographicum* shows intermediate specialization values and is probably underrepresented in our data set. The two remaining lichenicolous species are found only associated with a lichen host and are estimated to be highly specific (Table 5): *Sagediopsis fissurisedens* (MOTU 34) is found in asymptomatic and symptomatic samples of *Aspilidea myrinii*, and *Stigmidium eucline* seems to be restricted to the sample of *Varicellaria lactea* (Table 2). This divergence in specificity highlights the fact that lichenicolous fungi, as any trophic concept, also constitute a heterogenous assembly of

species with very different levels of specificity towards their hosts and also with very different ecological implications in functions in lichens as symbiotic systems.

## 4.3 | Symptomatic lichenicolous infections do not affect the mycobiome diversity

Contrary to our previous expectations based on SSCP analyses (Fleischhacker et al., 2015), sequence data revealed no clear differences in fungal diversity that could be attributable to the infection by individual, phenotypically distinct lichenicolous fungi. We also did not observe an alteration of the mycobiome composition that could reflect the entry of saprobiotic species on parasitized or damaged areas of the thallus. Differences in diversity might nevertheless exist consistently between host lichen species, possibly as a result of allelopathic effects by different secondary metabolites in different lichens (Lawrey, 1993; Torzilli, Mikelson, & Lawrey, 1999), or due to the diversity of microhabitats available in lichens with different anatomy and ultrastructure.

## 4.4 | The ecological components of lichen mycobiomes

Lichen mycobiomes clearly reflect the overlap of multiple ecological sets of taxa, which differ in their trophic association with lichen thalli. We identify three major ecological components: a) a generalist environmental pool, b) a lichenicolous/endolichenic pool and c) a pool of transient species.

The first set comprises generalist taxa common to the environmental pool of bio- and saprotrophic fungi. They are unspecific to their hosts and most likely feed on structural cell wall elements, extracellular exudates or secondary metabolites of plant, fungal or bacterial origin. In truth, at microscopic scales the difference between saprotrophy and biotrophy becomes diffuse. The relevance of this environmental pool is exemplified by the widespread presence of MOTUs identified as Tremellales. They are found in 23 of the 26 samples studied and form the predominant fraction of nine of them. According to their taxonomic assignments and subsequent confirmation alignments with reference sequences, these MOTUs do not represent known lichenicolous species of *Tremella*, but rather belong to species of Sirobasidiaceae, closer to the references of *Fibulobasidium* (Bandoni, 1979, 1998) than to *Sirobasidium*. The genus *Fibulobasidium* is found widespread on wood, bark and plant debris across geographic regions. Cannon and Kirk (2007) suggest that it may be parasitic on other fungi, an idea that is congruent with its presence in lichen-associated communities. In addition to *Fibulobasidium*, some of the less represented MOTUs of Capnodiales, Chaetothyriales and Botryosphaeriales in our data set also share environmental connections and lifestyles, being saprotrophs and endophytes. Most of them have melanized cell walls typical of stress-tolerant fungi. Oligotrophic, stress-tolerant fungi usually grow slowly and might be well adapted to survive in hostile conditions such as rock in alpine or arid habitats (Harutyunyan, Muggia, & Grube, 2008; Muggia et al., 2016).

The second species pool corresponds to the core of our study and is formed by lichenicolous and endolichenic fungi that grow and complete their life cycles (producing reproductive structures and spores) within lichen thalli. In general, they often belong to Capnodiales, Chaetothyriales and Botryosphaeriales, but unlike those species with clear environmental affinities, they are considered to be highly specialized. These species form the bulk of the reads and MOTUs found in the data set, and their most represented MOTUs are in turn those belonging to locally symptomatic taxa. Contrarily to the idea that lichenicolous fungi are extremely specialized towards their hosts, we observe very different levels of host specificity in MOTUs that are clearly identifiable as lichenicolous (Figure 3b, Table 5). In fact, six of the nine main lichenicolous MOTUs are widespread across host species in the data set (Table 5), and only three species, which are also underrepresented in the data set show a high predilection for a specific host. Coherently, MOTUs assigned to afore known lichenicolous species are unevenly distributed among samples: symptomatic thalli consistently have a high number of reads assignable to lichenicolous MOTUs, whereas asymptomatic thalli tend to render a small number of reads. However, the fact that specificity estimates are resilient to filtering and that some species are more widespread than others—despite of having a similar chance to be found as contaminants—support the interpretation of our results.

We are aware that retrieving sequences of a specific taxon from a microlichen sample does not necessarily mean that it plays an ecological role within its microbiome. Consequently, we argue that there is a third ecological component in the observed mycobiome community, formed by all species which disperse and possibly germinate on, among and within lichen thalli, but do not play a definite ecological role in the lichen community. Although some of the components of this third set may be just spurious sequences of propagules or spores or laboratory contaminants, we think that this third component also retrieves a complex spore and mycelium bank, in which lichens will work as suboptimal habitats or reservoirs which modulate and allow the regeneration of local fungal communities. In this respect, it has been long understood that ecosystems require the local availability of immature life stages to ensure the persistence of biological communities through time, an idea thoroughly discussed by Grubb (1977) for plant communities. In our case, immature stages (spores, propagules or mycelia) may be locally present on the surface of lichens but also between areoles and probably even intermingled within the structure of lichen thalli. The idea of having a propagule bank also explains the identification of lichen species other than the mycobionts of the analysed samples and of fungi and lichen species alien to the community in focus. Lichen thalli represent for these fungi suboptimal or unsuitable habitats where some species may be able to maintain an immature state within the thalli waiting for the chance to switch to a better habitat. Most of these species surely play no ecological role in the mycobiomes here analysed and have been thus considered spurious species.

## 5 | CONCLUSIONS

Summing up, we observe that the fungal communities that grow associated with lichen systems are indeed heterogeneous, taxonomic and ecological assemblages for which it is difficult to provide general statements. The openness of the lichen system itself and the obvious permeability of the thallus/substrate interface in microscopic crusts provide a further level of complexity in understanding which components of the mycobiome may be associated with different ecological compartments. However, the use of a taxonomically informed approach to the identification of locally occurring lichenicolous fungi and bipartite networks as main methodological framework enabled us to summarize global patterns and to discuss them on few focal taxa. The stability of our inferences to sample-specific threshold filtering, allowed us to ascertain that the observed lack of structure represents a solid background signal rather than a pervasive methodological noise in the form of spurious reads/contamination.

To eliminate the interference of spurious species in the mycobiome inferences, we devised a filtering approach in which read depth of clearly alien taxa was used as a criterion to choose what can be considered lichen-associated and what cannot. This type of criterion bases on the simple assumption that, if so much of the data set can be formed by alien species, everything below that threshold should be considered as noise and is also sample-dependent. Although we have introduced this denoising approach, we are aware that further refinements are needed to make the choice of the threshold more objective. The use of more stringent criteria tends to reduce network complexity and to interpret MOTUs as being exclusive for sample and host species. On the one side, this would be ecologically coherent; on the other, it would overlook the fact that lichenicolous fungi are (able to disperse) *everywhere, but the environment selects* those which play a role in the thalli of each lichen host (Baas Becking, 1934; de Wit & Bouvier, 2006).

Finally, we found here so far no clear evidence that the lichen mycobiome may affect the phenotype of its host, as shown by Spribille et al. (2016), but this possibility should be explored by further analyses, particularly with phenotypically heterogeneous lichen species complexes.


## ACKNOWLEDGEMENTS

The authors are grateful to the Austrian Science Fund for financial support (FWF projects P24114-B16 and P26359). We thank Ave Sujia for kindly providing a reference sequence of *Skyttea tephromelarum* and Josef Hafellner for constructive discussions.


## AUTHOR CONTRIBUTIONS

L.M. and M.G. conceived the study; L.M. coordinated the study; A.F. and L.M. carried out fieldwork and phylogenetic data analyses; T.K. extracted DNA and prepared samples for pyrosequencing; F.F.M. carried out the data processing, data analysis and graphic output; F.F.M., M.G. and L.M. wrote the manuscript; all authors approved the final version.

## DATA ACCESSIBILITY

Data files are uploaded to the NCBI Bioproject repository under the Accession Number PRJNA387391, including Biosamples (SAMN06947113–SAMN06947138) and Short read files (SRR5581750–SRR5581775). Original scripts and data files are made available at github.com/ferninfm/FFM_et_al_2017 (https://doi.org/10.5281/zenodo.582275).

## REFERENCES


Abarenkov, K., Nilsson, H. R., Larsson, K. H., Alexander, J. A., Eberhardt, U., Erland, S., Kõljalg, U.. (2010). The UNITE database for molecular identification of fungi–recent updates and future perspectives. *New Phytologist*, *186*, 281–285.

Almeida-Neto, M., Guimarães, P., Guimaraes, J. P. R., Loyola, R. D., & Ulrich, W. (2008). A consistent metric for nestedness analysis in ecological systems: Reconciling concept and measurement. *Oikos*, *117*, 1227–1239.

Amend, A. S., Seifert, K. A., & Bruns, T. D. (2010). Quantifying microbial communities with 454 pyrosequencing: Does read abundance count? *Molecular Ecology*, *19*, 5555–5565.

Arnold, A. E., Miadlikowska, J., Higgins, K. L., Sarvate, S. D., Gugger, P., Way, A., … Lutzoni, F. (2009). A phylogenetic estimation of trophic transition networks for ascomycetous fungi: Are lichens cradles of symbiotrophic fungal diversification? *Systematic Biology*, *58*, 283–297.

Aschenbrenner, I. A., Cernava, T., Berg, G., & Grube, M. (2016). Understanding microbial multi-species symbioses. *Frontiers in Microbiology*, *7*, 180.

Baas Becking, L. G. M. (1934). Geobiologie of inleiding tot de milieukunde. W.P. Van Stockum & Zoon, The Hague, the Netherlands.

Bandoni, R. J. (1979). *Fibulobasidium*: A new genus in the Sirobasidiaceae. *Canadian Journal of Botany*, *57*, 264–268.

Bandoni, R. J. (1998). On an undescribed species of *Fibulobasidium*. *Canadian Journal of Botany*, *76*, 1540–1543.

Bates, S. T., Cropsey, G. W., Caporaso, J. G., Knight, R., & Fierer, N. (2011). Bacterial communities associated with the lichen symbiosis. *Applied and Environmental Microbiology*, *77*, 1309–1314.

Bates, S. T., Walters, W. A., Knight, R., & Fierer, N. (2012). A pyrosequencing survey of lichen associated eukaryotes. *The Lichenologist*, *44*, 137–146.

Bellemain, E., Carlsen, T., Brochmann, C., Coissac, E., Taberlet, P., & Kauserud, H. (2010). ITS as an environmental DNA barcode for fungi: An in silico approach reveals potential PCR biases. *BMC microbiology*, *10*, 189.

Bengtsson-Palme, J., Ryberg, M., Hartmann, M., Branco, S., Wang, Z., Godhe, A., … Nilsson, R. H. (2013). ITSx: Improved software detection and extraction of ITS1 and ITS2 from ribosomal ITS sequences of fungi and other eukaryotes for use in environmental sequencing. *Methods in Ecology and Evolution*, *4*, 914–919.

Blaalid, R., Kumar, S., Nilsson, R. H., Abarenkov, K., Kirk, P. M., & Kauserud, H. (2013). ITS1 versus ITS2 as DNA metabarcodes for fungi. *Molecular Ecology Resources*, *13*, 218–224.

Blüthgen, N., Fründ, J., Vázquez, D. P., & Menzel, F. (2008). What do interaction network metrics tell us about specialization and biological traits. *Ecology*, *89*, 3387–3399.

Blüthgen, N., Menzel, F., & Blüthgen, N. (2006). Measuring specialization in species interaction networks. *BMC Ecology*, *6*, 1–12.

Blüthgen, N., Menzel, F., Hovestadt, T., Fiala, B., & Blüthgen, N. (2007). Specialization, constraints, and conflicting interests in mutualistic networks. *Current Biology*, *17*, 341–346.

Bragg, L., Stone, G., Imelfort, M., Hugenholtz, P., & Tyson, G. W. (2012). Fast, accurate error-correction of amplicon pyrosequences using Acacia. *Nature Methods*, *9*, 425–426.

del Campo, E. M., Catalá, S., Gimeno, J., Del Hoyo, A., Martínez-Alberola, F., Casano, L. M., … Barreno, E. (2013). The genetic structure of the cosmopolitan three-partner lichen *Ramalina farinacea* evidences the concerted diversification of symbionts. *FEMS Microbiology Ecology*, *83*, 310–323.

del Campo, E. M., Grimeno, J., De Nova, J. P. G., Casano, L. M., Gasulla, F., García-Breijo, F., & Reig-Armiñana Barreno, J. E. (2010). South European populations of Ramalina farinacea (L.) Ach. share different *Trebouxia* algae. In T. H. Nash III, L. Geiser, B. McCune, D. Triebel, A. M. F. Tomescu & W. B. Sanders (Eds.), *Biology of lichens - symbiosis, ecology, environmental monitoring, systematics and cyber applications*, *105*, (pp. 247–256). Stuttgart: Cramer in der Gebrüder Borntraeger Verlagsbuchhandlung, *Bibliotheca Lichenologica*.

Cannon, P. F., & Kirk, P. M. (2007). *Fungal families of the world*. London, UK: CAB International.

Cardinale, M., Vieira de Castro, J., Müller, H., Berg, G., & Grube, M. (2008). In situ analysis of the bacteria community associated with the reindeer lichen *Cladonia arbuscula* reveals predominance of Alphaproteobacteria. *FEMS Microbiology Ecology*, *66*, 63–71.

Casano, L. M., del Campo, E. M., García-Breijo, F. J., Reig-Armiñana, J., Gasulla, F., Del Hoyo, A., & Barreno, E. (2011). Two *Trebouxia* algae with different physiological performances are ever-present in lichen thalli of *Ramalina farinacea* - Coexistence versus competition? *Environmental Microbiology*, *13*, 806–818.

Chagnon, P. L., U'Ren, J. M., Miadlikowska, J., Lutzoni, F., & Elizabeth Arnold, A. (2016). Interaction type influences ecological network structure more than local abiotic conditions: Evidence from endophytic and endolichenic fungi at a continental scale. *Oecologia*, *180*, 181–191.

Crittenden, P. D., David, J. C., Hawksworth, D. L., & Campbell, F. S. (1995). Attempted isolation and success in the culturing of a broad spectrum of lichen-forming and lichenicolous fungi. *New Phytologist*, *130*, 267–297.

Dormann, C. F., Fründ, J., Bluthgen, N., & Gruber, B. (2009). Indices, graphs and null models: Analysing bipartite ecological networks. *The Open Ecology Journal*, *2*, 7–24.

Dormann, C. F., Gruber, B., & Fründ, J. (2008). Introducing the bipartite package: Analysing ecological networks. *R News*, *8*, 8–11.

Dunne, J. A., Williams, R. J., & Martinez, N. D. (2002). Food-web structure and network theory: The role of connectance and size. *Proceedings of the National Academy of Sciences of the United States of America*, *99*, 12917–12922.

Ertz, D., Diederich, P., Lawrey, J. D., Berger, F., Freebury, C. E. & Coppins, B. (2015). Phylogenetic insights resolve *Dacampiaceae* (*Pleosporales*) with polyphyletic: *Didymocyrtis* (*Pleosporales*, *Phaeosphaeriaceae*) with *Phoma*-like anamorphs resurrected and segregated from *Polycoccum* (*Trypetheliales*, *Polycoccaceae* fam. nov.). *Fungal Diversity*, *74*, 53–89.

Ertz, D., Heuchert, B., Braun, U., Freebury, C. E., Common, R. S., & Diederich, P. (2016). Contribution to the phylogeny and taxonomy of the genus *Taeniolella*, with a focus on lichenicolous taxa. *Fungal Biology*, *120*, 1416–1447.

Farrar, J. F. (1976). The lichen as an ecosystem: Observation and experiment. In D. H. Brown, D. L. Hawksworth & R. H. Bailey (Eds.), *Lichenology: Progress and problems* (pp. 385–406). London: Academic Press.

Fleischhacker, A., Grube, M., Kopun, T., Hafellner, J., & Muggia, L. (2015). Community analyses uncover high diversity of lichenicolous fungi in alpine habitats. *Microbial Ecology*, *70*, 348–360.

Fraley, C., & Raftery, A. E. (2002). Model-based clustering, discriminant analysis and density estimation. *Journal of the American Statistical Association*, *97*, 611–631.

Fraley, C., Raftery, A. E., Murphy, T. B., & Scrucca, L. (2012). *mclust Version 4 for R: Normal Mixture Modeling for Model-Based Clustering, Classification, and Density Estimation*. Technical Report No. 597, Department of Statistics, University of Washington.

Galeano, J., Pastor, J. M., & Iriondo, J. M. (2009). Weighted-Interaction Nestedness Estimator (WINE): A new estimator to calculate over frequency matrices. *Environmental Modelling and Software*, *24*, 1342–1346.

Gardes, M., & Bruns, T. D. (1993). ITS primers with enhanced specificity for basidiomycetes - application to the identification of mycorrhizae and rusts. *Molecular Ecology*, *2*, 113–118.

Girlanda, M., Isocrono, D., Bianco, C., & Luppi-Mosca, A. M. (1997). Two foliose lichens as microfungal ecological niches. *Mycologia*, *89*, 531–536.

Grubb, P. J. (1977). The maintenance of species-richness in plant communities: The importance of the regeneration niche. *Biological Reviews*, *52*, 107–145.

Grube, M., Cardinale, M., Vieira de Castro, J., Müller, H., & Berg, G. (2009). Species-specific structural and functional diversity of bacterial communities in lichen symbiosis. *The ISME Journal*, *3*, 1105–1115.

Grube, M., Cernava, T., Soh, J., Fuchs, S., Aschenbrenner, I., Lassek, C., & Berg, G. (2015). Exploring functional contexts of symbiotic sustain within lichen-associated bacteria by comparative omics. *The ISME Journal*, *9*, 412–424.

Gu, Z., Gu, L., Eils, R., Schlesner, M., & Brors, B. (2014). Circlize implements and enhances circular visualization in R. *Bioinformatics*, *30*, 2811–2812.

Hall, T. A. (1999). BioEdit: A user friendly biological sequence alignment editor and analysis program for Windows 95/98/NT. *Nucleic Acid Symposia Series*, *41*, 95–98.

Halwachs, B., Höftberger, J., Stocker, G., Snajder, R., Gorkiewicz, G., & Thallinger, G. G. (2013). High-throughput characterization and comparison of microbial communities. *Biomedizinische Technik* (Berlin).

Harutyunyan, S., Muggia, L., & Grube, M. (2008). Black fungi in lichens from seasonally arid habitats. *Studies in Mycology*, *61*, 83–90.

Hawksworth, D. L., & Honegger, R. (1994). The lichen thallus: A symbiotic phenotype of nutritionally specialized fungi and its response to gall producers. In: M. A. J. Williams (ed.), *Plant Galls. Organisms, interactions, populations. The systematics association special volume* (pp. 77–98), Oxford: Clarendon Press.

Henning, C. (2015). Package fpc: Flexible procedures for clustering. Retrieved from https://cran.r-project.org/web/packages/fpc/fpc.pdf.

Hodkinson, B. P., & Lutzoni, F. M. (2010). A microbiotic survey of lichen-associated bacteria reveals a new lineage from the Rhizobiales. *Symbiosis*, *49*, 163–180.

Huson, D., Mitra, S., & Ruscheweyh, H. (2011). Integrative analysis of environmental sequences using MEGAN4. *Genome Research*, *21*, 1552–1560.

Katoh, S. (2013). MAFFT multiple sequence alignment software version 7: Improvements in performance and usability. *Molecular Biology and Evolution*, *30*, 772–780.

Kozich, J. J., Westcott, S. L., Baxter, N. T., Highlander, S. K., & Schloss, P. D. (2013). Development of a dual-index sequencing strategy and curation pipeline for analyzing amplicon sequence data on the MiSeq Illumina sequencing platform. *Applied and Environmental Microbiology*, *79*, 5112–5120.

Lawrey, J. D. (1993). Chemical ecology of *Hobsonia christiansenii*, a lichenicolous hyphomycete. *American Journal of Botany*, *80*, 1109–1113.

Lawrey, J. D., & Diederich, P. (2003). Lichenicolous fungi : Interactions, evolution, and biodiversity. *The Bryologist*, *106*, 80–120.

Lawrey, J. D., & Diederich, P. (2017). Lichenicolous fungi – worldwide checklist, including isolated cultures and sequences available. Retrieved from: http://www.lichenicolous.net.

Lawrey, J. D., Etayo, J., Dal-Forno, M., Driscoll, K. E., & Diederich, P. (2015). Phylogenetic insights resolve Dacampiaceae (Pleosporales) as polyphyletic: *Didymocyrtis* (Pleosporales, Phaeosphaeriaceae) with *Phoma*-like anamorphs resurrected and segregated from *Polycoccum* (Trypetheliales, Polycoccaceae fam. nov.). *Fungal Diversity*, *74*, 53–89.

Lawrey, J. D., Zimmermann, E., Sikaroodi, M., & Diederich, P. (2016). Phylogenetic diversity of bulbil-forming lichenicolous fungi in Cantharellales including a new genus and species. *The Bryologist*, *119*, 341–349.

Mahé, F., Rognes, T., Quince, C., de Vargas, C., & Dunthorn, M. (2014). Swarm: Robust and fast clustering method for amplicon-based studies. *PeerJ*, *2*, e593.

Muggia, L., Fleischhacker, A., Kopun, T., & Grube, M. (2016). Extremotolerant fungi from alpine rock lichens and their phylogenetic relationships. *Fungal Diversity*, *76*, 119–142.

Muggia, L., & Grube, M. (2010). Fungal composition of lichen thalli assessed by single strand conformation polymorphism. *The Lichenologist*, *42*, 1–13.

Muggia, L., Kopun, T., & Ertz, D. (2015). Phylogenetic placement of the lichenicolous, anamorphic genus *Lichenodiplis* and its connection to *Muellerella*-like teleomorphs. *Fungal Biology*, *119*, 1115–1128.

Muggia, L., Perez-Ortega, S., Kopun, T., Zellnig, G., & Grube, M. (2014). Photobiont selectivity leads to ecological tolerance and evolutionary divergence in a polymorphic complex of lichenized fungi. *Annals of Botany*, *114*, 463–475.

Oksanen, J. (2015). *vegan : ecological diversity*. Retrieved from https://cran.r-project.org/web/packages/vegan/ vignettes/diversity-vegan.pdf

Oksanen, J., Blanchet, F. G., Kindt, R., Legendre, P., Minchin, P. R., O' Hara, R. B., Simpson, G. L., Solymos, P., Henry, M., Stevens, H., & Wagner, H. (2015). *vegan: Community Ecology Package*. R package version 2.2-1. Retrieved from http://CRAN.R-project.org/package=vegan

Petrini, O., Hake, U., & Dreyfuss, M. M. (1990). An analysis of fungal communities isolated from fruticose lichens. *Mycologia*, *82*, 444–451.

Piercey-Normore, M. D., & Depriest, P. T. (2001). Algal switching in lichen symbioses. *American Journal of Botany*, *88*, 1490–1498.

Poisot, T., Bever, J. D., Nemri, A., Thrall, P. H., & Hochberg, M. E. (2011). A conceptual framework for the evolution of ecological specialisation. *Ecology Letters*, *14*, 841–851.

Prillinger, H., Kraepelin, G., Lopandic, K., Schweigkofler, W., Molnar, O., Weigang, F., & Dreyfuss, M. M. (1997). New species of *Fellomyces* isolated from epiphytic lichen species. *Systematic and Applied Microbiology*, *20*, 572–584.

Printzen, C., Fernández-Mendoza, F., Muggia, L., Grube, M., & Berg, G. (2012). Alphaproteobacterial communities in geographically distant populations of the lichen *Cetraria aculeata*. *FEMS Microbiology Ecology*, *82*, 316–325.

R Development Core Team (2011). R: A Language and Environment for Statistical Computing.

Rodríguez-Gironés, M. A., & Santamaría, L. (2006). A new algorithm to calculate the nestedness temperature of presence-absence matrices. *Journal of Biogeography*, *33*, 924–935.

Schmidt, P. A., Balint, M., Greshake, B., Bandow, C., Roembke, J., & Schmit, I. (2013). Illumina metabarcoding of a soil fungal community. *Soil Biology and Biochemistry*, *65*, 128–132.

Schoch, C. L., Seiferth, K. A., Huhndorf, S., Robert, V., Spouge, J. L., Levesque, C. A., Chen, W., & Fungal Barcoding Consortium. (2012). Nuclear ribosomal internal transcribed spacer (ITS) region as a universal DNA barcode marker for Fungi. *Proceedings of the National Academy of Science*, *109*, 6241–6246.

Silvestro, D., & Michalak, I. (2011). raxmlGUI: A graphical front-end for RAxML. *Organisms Diversity & Evolution*, *12*, 335–337.

Spribille, T., Tuovinen, V., Resl, P., Vanderpool, D., Wolinski, H., Aime, M. C., … McCutcheon, J. P. (2016). Basidiomycete yeasts in the cortex of ascomycete macrolichens. *Science*, *353*, 488–492.

Stamatakis, A. (2004). Distributed and parallel algorithms and systems for inference of huge phylogenetic trees based on the maximum likelihood method. Doctoral Thesis, Munich.

Stamatakis, A. (2006). RAxML-VI-HPC: Maximum likelihood-based phylogenetic analyses with thousands of taxa and mixed models. *Bioinformatics*, *22*, 2688–2690.

Stenroos, S., Stocker-Wörgötter, E., Yoshimura, I., Myllys, L., Thell, A., & Hyvönen, J. (2003). Culture experiments and DNA sequence data confirm the identity of *Lobaria* photomorphs. *Canadian Journal of Botany*, *81*, 232–247.

Torzilli, A. P., Mikelson, P. A., & Lawrey, J. D. (1999). Physiological effect of lichen secondary metabolites on the lichen parasite *Marchandiomyces corallinus*. *The Lichenologist*, *31*, 307–314.

Tylianakis, J. M., Tscharntke, T., & Lewis, O. T. (2007). Habitat modification alters the structure of tropical host-parasitoid food webs. *Nature*, *445*, 202–205.

U'Ren, J. M., Lutzoni, F. M., Miadlikowska, J., & Arnold, A. E. (2010). Community analysis reveals close affinities between endophytic and endolichenic fungi in mosses and lichens. *Microbial Ecology*, *60*, 340–353.

U'Ren, J. M., Lutzoni, F., Miadlikowska, J., Laetsch, A. D., & Arnold, E. (2012). Host and geographic structure of endophytic and endolichenic fungi at a continental scale. *American Journal of Botany*, *99*, 898–914.

U'Ren, J. M., Riddle, J. M., Monacell, J. T., Carbone, I., Miadlikowska, J., & Arnold, A. E. (2014). Tissue storage and primer selection influence pyrosequencing-based inferences of diversity and community composition of endolichenic and endophytic fungi. *Molecular Ecology Resources*, *14*, 1032–1048.

Wang, Y., Zheng, Y., Wang, X., Wei, X., & Wei, J. (2016). Lichen-associated fungal community in *Hypogymnia hypotrypa* (Parmeliaceae, Ascomycota) affected by geographic distribution and altitude. *Frontiers in Microbiology*, *7*, 1231.

Wedin, M., Maier, S., Fernandez-Brime, S., Cronholm, B., Westberg, M., & Grube, M. (2015). Microbiome change by symbiotic invasion in lichens. *Environmental Microbiology*, *18*, 1428–1439.

White, T. J., Bruns, T., Lee, S., & Taylor, J. W. (1990). Amplification and direct sequencing of fungal ribosomal RNA genes for phylogenetics. In M. A. Innis, D. H. Gelfand, J. J. Sninsky, & T. J. White (Eds.), *PCR protocols: A guide to methods and applications* (pp. 315–322). New York: Academic Press Inc.

de Wit, R., & Bouvier, T. (2006). "Everything is everywhere, but, the environment selects"; what did Baas Becking and Beijerinck really say? *Environmental Microbiology*, *8*, 755–758.

Zhang, Z., Schwartz, S., Wagner, L., & Miller, W. (2000). A greedy algorithm for aligning DNA sequences. *Journal of Computational Biology*, *7*, 203–214.

Zhang, T., Wei, X.-L., Zhang, Y.-Q., Liu, H.-Y., & Yu, L.-Y. (2015). Diversity and distribution of lichen-associated fungi in the Ny-Ålesund Region (Svalbard, High Arctic) as revealed by 454 pyrosequencing. *Scientific Reports*, *5*, 14850.